Javelin-, Hockey Stick-, and Boomerang-Shaped Liquid Crystals. Structural Variations on *p*-Quinquephenyl[†]

Theo J. Dingemans,[‡] N. Sanjeeva Murthy,[§] and Edward T. Samulski*

Department of Chemistry, University of North Carolina at Chapel Hill,
*Chapel Hill, North Carolina 27599-3290*

Received: March 7, 2001

The ramifications of changing molecular geometry in a series of all-aromatic liquid crystals derived from *p*-quinquephenyl are reported. Substituting heterocyclic rings such as thiophene, oxadiazole, oxazole, or 1,3-phenylene into the *p*-quinquephenylene core affects molecular shape changes via the substituent's exocyclic bond angle. In general, we found that introducing nonlinearity into molecules depresses the melting transition temperature. The symmetric (boomerang-shaped) molecules, 2,5-bisbiphenyl-4-*yl*-1,3,4-oxadiazole, 2,5-bisbiphenyl-4-*yl*-oxazole, and 1,3-bisbiphenyl-4-*yl*-benzene, melt into isotropic phases showing small monotropic mesophases. By contrast, the asymmetric (hockey stick-shaped) mesogens, 2-terphenyl-4-*yl*-5-phenyl thiophene and 2-terphenyl-4-*yl*-5-phenyl-1,3,4-oxadiazole, exhibit more stable enantiotropic liquid crystalline phases. The hockey stick-shaped mesogens exhibit a smectic phase as well as a nematic phase. High-temperature X-ray determination of the smectic layer spacing gives an unambiguous picture of interdigitated, bilayerlike supramolecular architecture in the smectic phase. There are associated changes in the mesogen's electrostatic profile when a heterocycle is introduced into the quinquiphenylene framework (e.g., conjugation is perturbed). Our findings suggest that steric packing considerations dominate the phase preferences (nematic versus smectic phases). However, electronic considerations (conjugation) appear to control the range of mesomorphism in this new family of nonlinear liquid crystals.

Introduction

Anisometric, rodlike- or disklike-shaped molecules are prerequisite for liquid crystal formation because steric packing considerations play an important role in this curious state of soft matter.[1] But electrostatic interactions are also important as these are responsible for condensed phases generally, and anisotropic electrostatic interactions may reinforce packing preferences in liquid crystals. Packing and electrostatics are usually optimized in molecular crystals and the resulting intermolecular cohesion determines the crystal's fusion temperature. If the thermal energy in the melt phase is too high, it may overwhelm the delicate interplay between (anisotropic) attractive forces and dynamic packing preferences needed for propagating long-range orientational order, the signature of liquid crystallinity.

Generally, the interplay between intermolecular attraction and packing is obscured by the molecular structures of most liquid crystals (mesogens). Typically, the structural building-blocks of mesogens—heteroatom-containing linkages (ether, ester, azoxy, etc.), cyclic aliphatic and/or aromatic rings, variable conjugation within the "mesogenic core," and pendant fluoro and/or alkyl chains—result in a complex distribution of electron density along the molecular framework. As a result, a mesogen's "electrostatic profile" may not be described in a simple, additive fashion. Also, facile characterization of most mesogen shapes is precluded by internal molecular flexibility of its structural

building blocks. However, the liquid crystal *p*-quinquephenyl (PPPPP; **I**, n = 5)

(I)
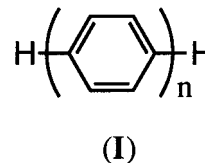
is an exception having a well-defined, rodlike shape with minimal internal flexibility (only "free" rotation about its *para*-substituted phenyl rings), and an essentially uniform distribution of electron density. First investigated by Vorländer in 1927,[2] This class of mesogens was examined by Flory et al.[3] in the early 1980s; PPPPP is the simplest rodlike (calamitic) mesogen known. As there is no ambiguity about PPPPP's shape nor its electrostatic profile, if one could independently change the geometry of the simple PPPPP mesogen without perturbing its electrostatic profile, it might be possible to quantify the relative importance of steric and electrostatic contributions to liquid crystal formation—phase preferences (nematic versus smectic) and phase stability (the mesophase thermal window). Herein we report structural variations in the parent mesogen PPPPP in order to learn more about the relative importance of steric and electrostatic contributions to liquid crystallinity.

In actuality the rodlike shape of PPPPP can be altered albeit only with unavoidable changes in its electrostatic profile. We try to minimize changes in the latter by considering structural variations of *p*-quinquephenyl wherein a single *para*-substituted phenylene is replaced with an aromatic (2,5-substituted) heterocycle (e.g., thiophene, oxadiazole, or oxazole). Introducing
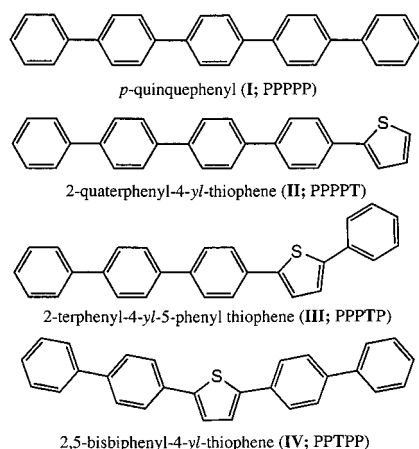

SCHEME 1: Javelin-, Hockey Stick-, and Boomerang-Shaped Mesogens Derived from Insertion of 2,5-Substituted Thiophene into the *p*-Quinquephenyl Molecular Framework; Molecular Dipole Moments Are $\mu \approx 0$ D for PPPPP and ~ 0.5 D for II, III, and IV

p-quinquephenyl (**I**; PPPPP)

2-quaterphenyl-4-*yl*-thiophene (**II**; PPPPT)

2-terphenyl-4-*yl*-5-phenyl thiophene (**III**; PPPTP)

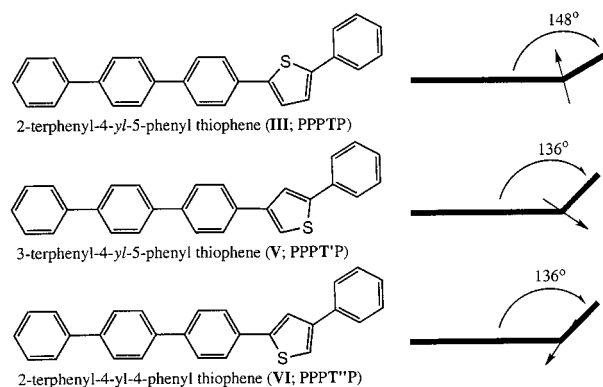2,5-bisbiphenyl-4-*yl*-thiophene (**IV**; PPTPP)

the heterocycle **X** (= thiophene, oxadiazole, or oxazole) into the parent PPPPP molecules yields new, nonlinear mesogens having well-defined shapes, e.g., linear mesogens with distinguishable ends that we designate as "javelins" (PPPP**X**), asymmetric bent "hockey sticks" (PPP**X**P), and "boomerang-shaped" mesogens (PP**X**PP). These substitutions in the *p*-phenylene core change the molecular shape because the exocyclic bond angle in **X** is decreased—from 180° in *p*-phenylene to 148°, 136°, or 120 °, respectively, for thiophene, oxadiazole, and *m*-phenylene. Although the mesogen's electronic profile will be altered by such substitutions (for example, the PPPPP electronic conjugation is interrupted in PPP**X**P and in PP**X**PP when **X** = *m*-phenylene), one can nevertheless derive generic trends from the experimental data about how mesogen shape influences mesophase stability and phase type. In this way we try to deconvolve the electrostatic and steric contributions in liquid crystals.

We report how the liquid crystalline behavior is modified in these new five-ring mesogens relative to the classical calamitic mesogen PPPPP. We found that the PPP**X**P isomers constitute a new class of smectic-A liquid crystals. We are especially interested in the supramolecular packing in the crystal and liquid crystalline phases of hockey stick-shaped PPP**X**P; we report the smectic layer thickness using high-temperature X-ray diffraction. As the PPP**X**P molecular dimensions can be determined without ambiguity (unlike for traditional thermotropic mesogens containing flexible and/or interdigitated alkyl chains), a detailed molecular interpretation of the packing arrangement in this new smectic-A material is possible.
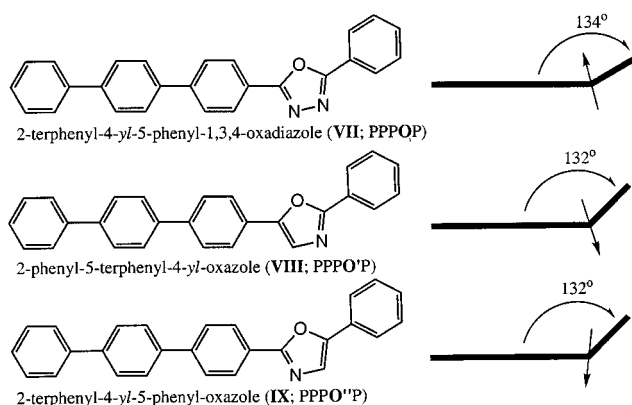
Target Mesogens. We have targeted three series of structural variations on quinquephenyl in an effort to change the shape of the parent mesogen PPPPP. We investigate the role of mesogen geometry for (conjugated) five-ring molecules by introducing a 2,5-substituted heterocycle into the PPPPP framework.

Quaterphenyl-thiophenes. In the first series, the thiophene heterocycle (**T**) is translated from a terminal "1" position (PPPP**T**) to the "2" position (PPPP**T**P), and finally to the center forming a symmetric five-ring molecule (PP**T**PP). In 2-quaterphenyl-4-*yl*-thiophene (PPPP**T**; **II**) with the heterocycle at one end, the linear shape is maintained and conjugation from the *para*-linked phenylenes persists into the thiophene ring; the latter ring's heteroatom introduces a polar tip (~ 1 D dipole moment)

SCHEME 2: Thiophene Isomers of PPPTP (III) Showing Variable Dipole Directions and Exocyclic Bond Angles; μ = 0.47 D, 0.53 D, and 0.54 D for III, V, and VI, Respectively

2-terphenyl-4-*yl*-5-phenyl thiophene (**III**; PPPTP)

3-terphenyl-4-*yl*-5-phenyl thiophene (**V**; PPP**T'**P)

2-terphenyl-4-yl-4-phenyl thiophene (**VI**; PPP**T''**P)

SCHEME 3: Oxadiazole and Oxazole Analogues PPPXP. The Size and Direction of the Electrostatic Dipole Moment Varies (μ = 4.03, 1.75, and 1.51 D for VII, VIII, and IX, Respectively). The Exocyclic Bond Angle Is Unchanged in This Series
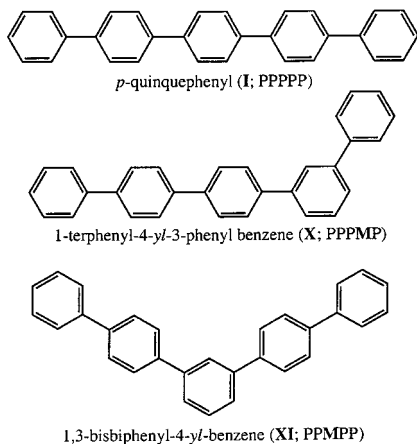

2-terphenyl-4-*yl*-5-phenyl-1,3,4-oxadiazole (**VII**; PPP**O**P)

2-phenyl-5-terphenyl-4-*yl*-oxazole (**VIII**; PPP**O'**P)

2-terphenyl-4-*yl*-5-phenyl-oxazole (**IX**; PPP**O''**P)

to give a "javelin"-shaped molecule. For the molecule 2-terphenyl-4-*yl*-5-phenyl thiophene (PPP**T**P; **III**) the heterocycle introduces shape asymmetry. The resulting "hockey stick" shape should profoundly influence packing without a major change in the molecule's electrostatic profile. Thiophene in the "3" position [-2,5-bisbiphenyl-4-*yl*-thiophene (PP**T**PP; **IV**)]is a symmetric, conjugated molecule with an overall "boomerang" shape.

Scheme 2 displays a related series wherein we "rotate" the thiophene moiety to give isomers of the hockey stick-shaped molecule. For the 3,5-thiophene isomer (**V**) and the 2,4-thiophene isomer (**VI**) denoted PPP**T'**P and PPP**T''**P, several things change when the substitution pattern changes: (1) The exocyclic bond angle decreases by 10° (from 148° to 138° as determined by AM1 calculations);[4] (2) The orientation of the electrostatic dipole moment associated with the sulfur atom in thiophene changes; The magnitude of the dipole moment—along the C_2 axis of 2,5-substituted thiophenes—is 0.52 D in thiophene,[5] and 0.92 D in 2,5-diphenyl thiophene.[6] (3) The conjugation is curtailed at the thiophene ring (similar to inserting a *meta*-substituted phenyl into quinquephenyl).

Quaterphenyl-oxadiazoles. We have also targeted more extreme exocyclic bond angles and correspondingly larger electrostatic dipole moments in modified PPP**X**P "hockey sticks" having **X** = oxadiazole (**VII**; PPP**O**P). This class of molecules may also have the dipole rotated by breaking the symmetry of the oxadiazole ring, i.e., using **X** = oxazole heterocycles (**VIII**

SCHEME 4: *m*-Phenylene Analogues of *p*-Quinquephenyl; $\mu \approx 0$ D (0.08 D) for All of These Isomers

p-quinquephenyl (**I**; PPPPP)

1-terphenyl-4-*yl*-3-phenyl benzene (**X**; PPPMP)

1,3-bisbiphenyl-4-*yl*-benzene (**XI**; PPMPP)

and **IX** or PPPO′P and PPPO″P, respectively). This series of potential mesogens is shown in Scheme 3. In addition to larger and variably oriented dipole moments, in contrast with thiophene, the exocyclic bond angle remains nearly the same on going from the oxadiazole PPPOP (136°) to the oxazole (134°) derivatives PPPO′P and PPPO″P.[7−9] This feature allows us to study the effect of the size and direction of the electrostatic dipole moment with a minimum change in overall molecular shape. For reference purposes, the dipole moment associated with oxadiazole in 2,5-diphenyl-1,3,4-oxadiazole is 3.86 D[9] and that associated with oxazole in 2,5-diphenyl-oxazole is 1.55 D.[8] Also, there is a marked change in the aromaticity on going from the symmetric oxadiazole ring in PPPOP to the oxazole ring (PPPO′P and PPPO″P). The oxazole heterocycle has a more dienic character, which leads to reduced conjugation in the latter two mesogens[10] relative to 2,5-diphenyl-1,3,4-oxadiazole, where the conjugation is found to be similar to that in polyphenylenes.[11] So in this series we have constant geometry, variable conjugation, and variable electrostatic dipole moment orientation (and magnitude). But this is convolved with polarizability differences that can reinforce anisotropic interactions, i.e., we anticipate changes in the attractive interactions in melts of PPPO′P (and PPPO″P) relative to PPPOP.

Nonlinear Quinquephenyls. The final series targets 1,3- or *m*-phenylene-based quinquephenyls. This is the most extreme of the nonlinear-shaped molecules having a 120° exocyclic bond angle at the 1,3-substituted ring. The routes to these *m*-phenylene derivatives PPPMP and PPMPP (**X** and **XI**) are shown in Scheme 4. In this series the geometrical changes relative to

PPPPP are greatest, and there is a negligible dipole moment change when going from **X** = P to **X** = M. However the conjugation is interrupted at the *meta*-substituted phenyl ring and these nonpolar molecules have reduced polarizability anisotropies relative to PPPPP.

Synthetic Strategy

Attempts have been made in the past to synthesize different isomers of PPPPP (**I**) by pyrolysis of *p*-terphenyl[12] or through the Ullmann reaction.[13,14] However, both routes gave complex mixtures of products that were hard to separate and identify. To circumvent these problems we have adopted the Suzuki cross-coupling strategy which has been proven to be very successful in the synthesis of multi-aryl mesogenic systems by Hird et al.[15] This technique allows the synthesis of complex substitution patterns and only requires appropriate aryl bromides and arylboronic acids which are coupled in the presence of a palladium(0) catalyst and a base. This chemistry usually proceeds in high yields and with no significant side reactions.

The synthesis of some common intermediates such as 4-biphenylboronic acid (**2**) and 4-bromo-*p*-terphenyl (**4**) is illustrated in Scheme 5. Since 4-bromo-*p*-terphenyl (**4**) is a key intermediate and needed to be of high purity we decided to synthesize this compound through the cross-coupling of 1-bromo-4-iodobenzene (**3**) and 4-biphenylboronic acid (**2**). The coupling in this case was, as expected, highly specific toward the iodo coupling site.[15]

Scheme 6 illustrates the synthesis of the first series of thiophene-modified quinquephenyls in which thiophene translates through the molecule. The symmetric compounds (**I**) and (**IV**) were synthesized using 4-biphenylboronic acid (**2**) and the appropriate aryl dibromide. The asymmetric compounds (**II**) and (**III**) were obtained through multiple coupling reactions. In the first step, the intermediate aryl thiophene was synthesized and converted into its corresponding boronic acid and was subsequently coupled with 4-bromo-*p*-terphenyl (**4**).

Rotating the thiophene moiety in 2-terphenyl-4-*yl*-5-phenyl thiophene (**III**) required more complex aryl thiopheneboronic acid intermediates, as can be seen in Scheme 7.
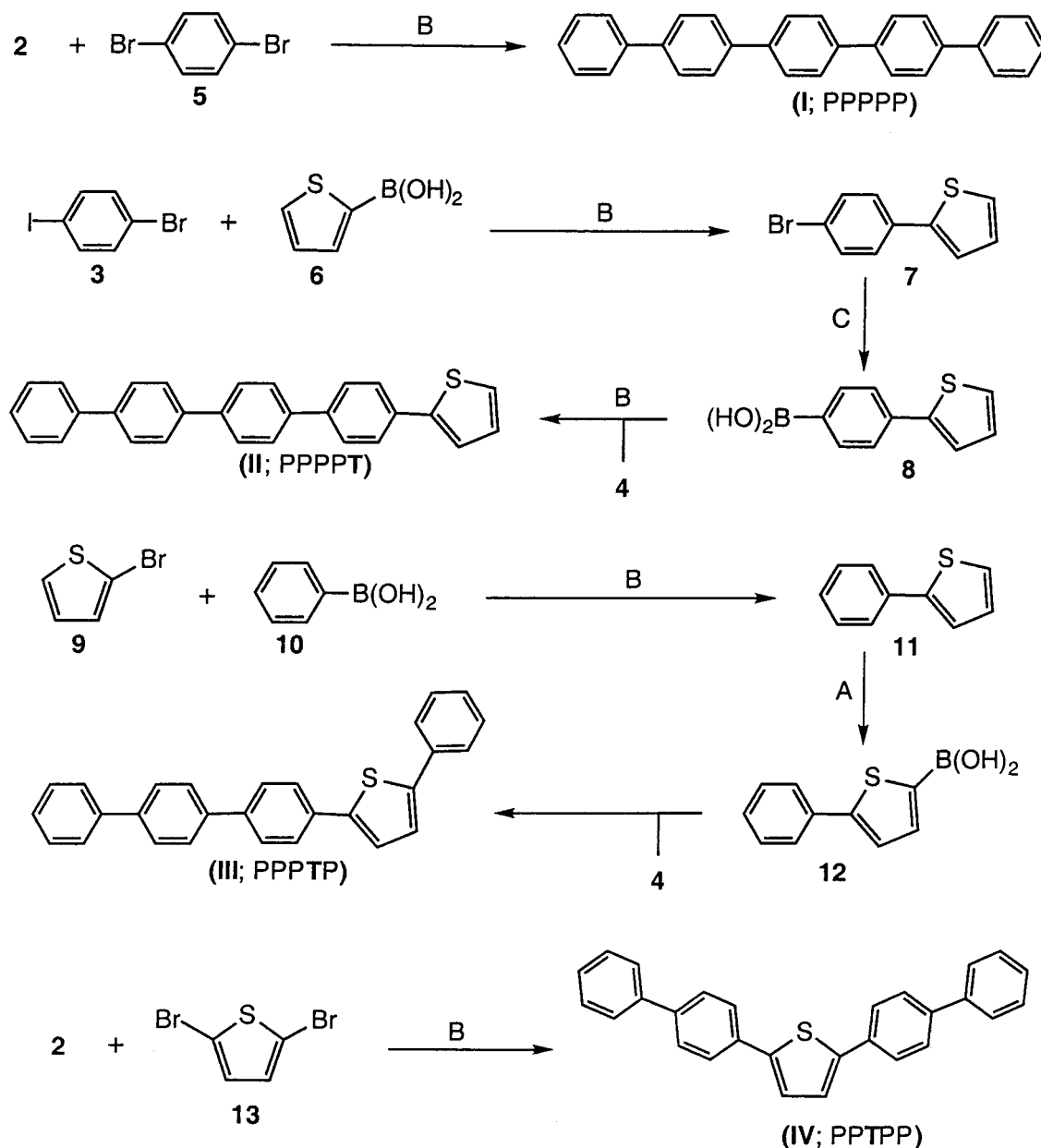
4-Bromo-2-phenyl-thiophene (**15**) was made according to a procedure published by Gjøs and Gronowitz.[16] In the first step, lithiation of 2,4-dibromothiophene at −78° C takes place predominantly at the 2-position. The 2-lithio intermediate was quenched in cyclohexanone and after hydrolysis, the intermediate tertiary alcohol was dehydrated to yield 4-bromo-2-(1-cyclohexenyl) thiophene. This compound was aromatized in the presence of dichlorodicyanoquinone (DDQ) and gave the desired

SCHEME 5: Synthesis of Common Intermediates; 4-Biphenylboronic Acid (2) and 4-Bromo-*p*-terphenyl (4)
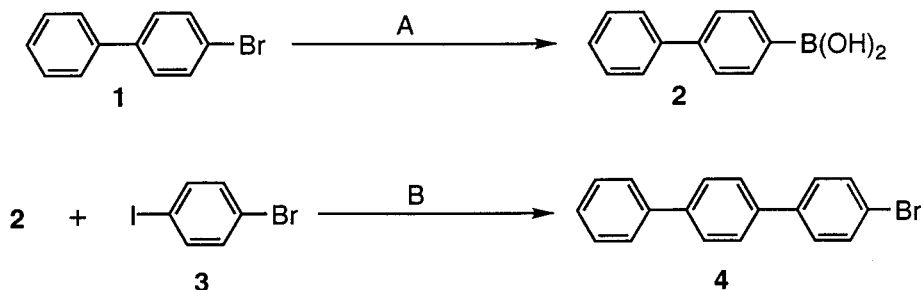
A (i) *n*-BuLi, THF (-78 °C); (ii) (MeO)$_3$B, THF (-78 °C); (iii) 10% HCl
B Pd(PPh$_3$)$_4$, 1,2-dimethoxyethane, 2M-Na$_2$CO$_3$

SCHEME 6: The Synthetic Routes to the 2,5-Thiophene-Modified *p*-Quinquephenyls (I−IV)

A (i) *n*-BuLi, THF (-78 °C); (ii) (MeO)₃B, THF (-78 °C); (iii) 10% HCl

B Pd(PPh₃)₄, 1,2-dimethoxyethane, 2M-Na₂CO₃

C (i) Mg, THF; (ii) (MeO)₃B, THF (-78 °C); (iii) 10% HCl

4-bromo-2-phenyl-thiophene (**15**), which was converted to its corresponding boronic acid (**16**). Coupling the boronic acid with 4-bromo-*p*-terphenyl (**4**) gave 3-terphenyl-4-*yl*-5-phenyl thiophene (**V**).

2-Bromo-4-phenyl-thiophene (**19**) was available through bromination of 3-phenyl thiophene as reported by Gjøs et al.[17] When carried out in acidic acid, bromination takes place predominately at the 5-position. Coupling of the corresponding boronic acid (**20**) with 4-bromo-*p*-terphenyl (**4**) gave 2-terphenyl-4-*yl*-4-phenyl thiophene (**VI**).

The oxadiazole (**VII**)- and oxazole (**VIII** and **IX**)-based liquid crystals were synthesized using a different approach and it is shown in Scheme 8. Instead of coupling 4-bromo-*p*-terphenyl (**4**) with the appropriate heterocyclic boronic acid we decided to synthesize the 2-(4-bromophenyl)-5-phenyl heterocycle and

couple this with 4-biphenylboronic acid (**2**). This way we could avoid complex synthetic steps that would otherwise be required to obtain the heterocyclic aryl bromides and their corresponding boronic acids.

2-(4-Bromophenyl)-5-phenyl-1,3,4-oxadiazole (**23**) was synthesized using the procedure published by Wang et al.[18] *p*-Bromobenzoyl chloride (**21**) was coupled with benzoic hydrazide (**22**) under basic conditions and the resulting amide was treated with POCl₃ to give the 2-(4-bromophenyl)-5-phenyl-1,3,4-oxadiazole (**23**).

5-(4-Bromophenyl)-2-phenyl-oxazole (**26**) and 2-(4-bromophenyl)-5-phenyl-oxazole (**29**) were prepared according to a similar procedure as reported by Hayes et al.[19]

The synthesis of compounds (**X**) and (**XI**) is shown in Scheme 9. The coupling of the 3-biphenylboronic acid (**31**) with

SCHEME 7: The Synthetic Routes to the 3,5- and 2,4-Thiophene Isomers of 2-Terphenyl-4-*yl*-5-phenyl Thiophene (V and VI)
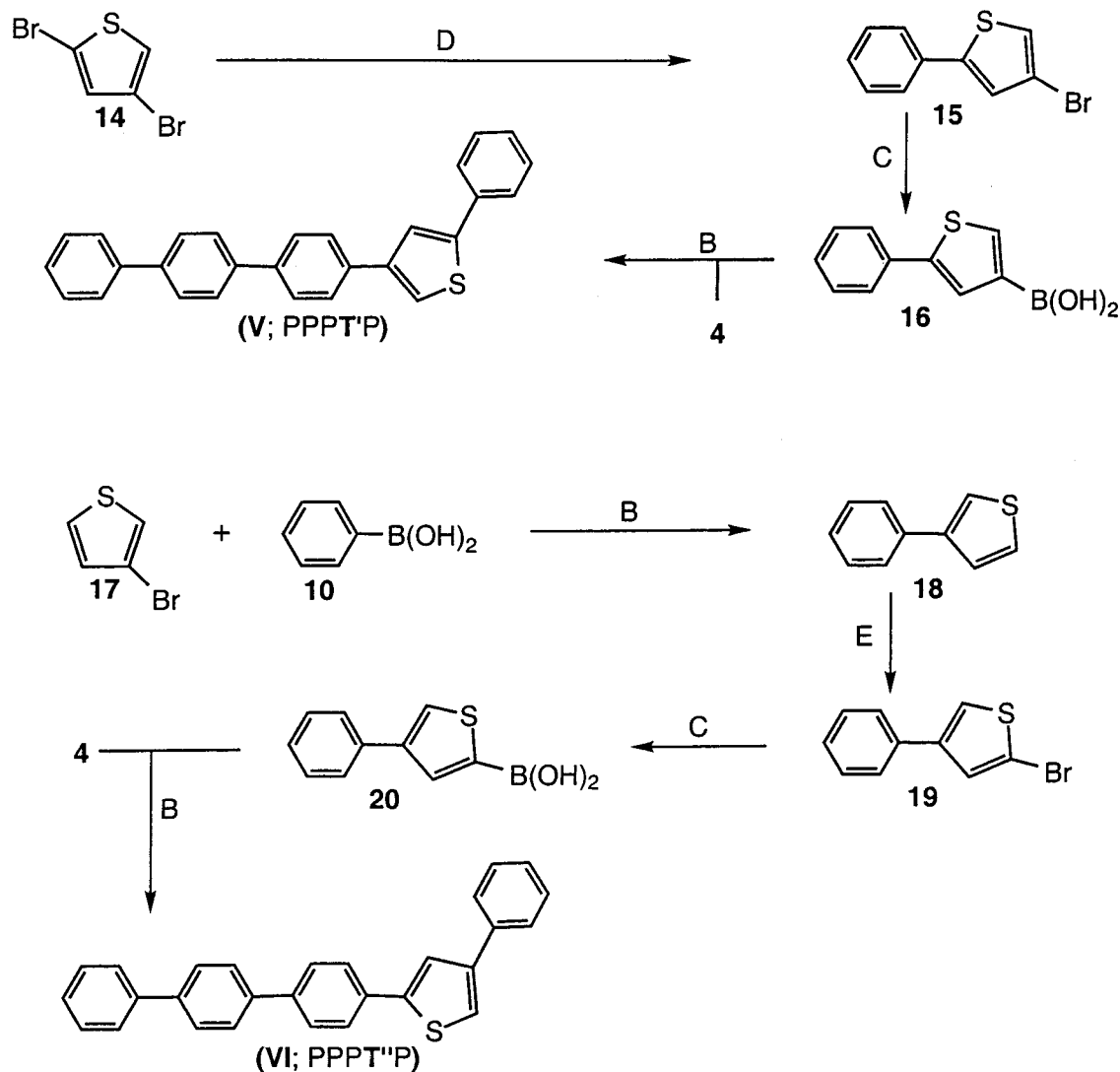
B Pd(PPh$_3$)$_4$, 1,2-dimethoxyethane, 2M-Na$_2$CO$_3$

C (i) Mg, THF; (ii) (MeO)$_3$B, THF (-78 °C); (iii) 10% HCl

D (i) *n*-BuLi, Et$_2$O; (ii) cyclohexanone; (iii) 6N HCl; (iv) DDQ, Benzene

E Br$_2$, HOAc

4-bromo-*p*-terphenyl (**4**) gave 1-terphenyl-4-*yl*-3-phenyl benzene (**X**) and coupling of 4-biphenylboronic acid (**2**) with 1,3-dibromobenzene (**32**) gave 1,3-bisbiphenyl-4-*yl*-benzene (**XI**).

Results

Thermal Analysis. The DSC results of a series of thiophene-based model compounds are presented in Table 1.

The transition temperatures are lowered dramatically when nonlinearity is introduced into the PPPPP molecular framework. This geometrical trend—depressing transition temperatures—is exaggerated when thiophene is translated to the center of the *p*-quinquephenyl core. Replacing the terminal phenyl group with a thiophene moiety, PPPPT (**II**), results in the broadening of the nematic mesophase relative to PPPPP. Since this replacement does not seriously perturb the overall shape of the parent compound, the increased orientational entropy (from the now

distinguishable ends of the javelin-shaped mesogen) probably contributes to the mesophase stabilization in PPPPT.

We find a surprising observation for thiophene in the 2 position: PPPTP (**III**) has an asymmetric structure that resembles the shape of a hockey stick yet it exhibits a mesophase range that is much broader than the parent compound, *p*-quinquephenyl, and moreover, PPPTP forms both SmA and N phases. The DSC trace of PPPTP (second heating, 10 °C/min) is shown in Figure 1. To our knowledge this is only the second example of a wholly aromatic liquid crystal that forms a SmA phase. *p*-Sexiphenyl (**I**, n = 6) was reported to have a SmA phase at very high temperatures (>500 °C) but thermal decomposition inhibited a detailed characterization of the mesophases.[20]

Placing the thiophene heterocycle into the central position, PPTPP (**IV**), results in an overall boomerang shape that

SCHEME 8: The Synthetic Routes to the Oxadiazole (VII) and Oxazole (VIII and IX) Mesogens
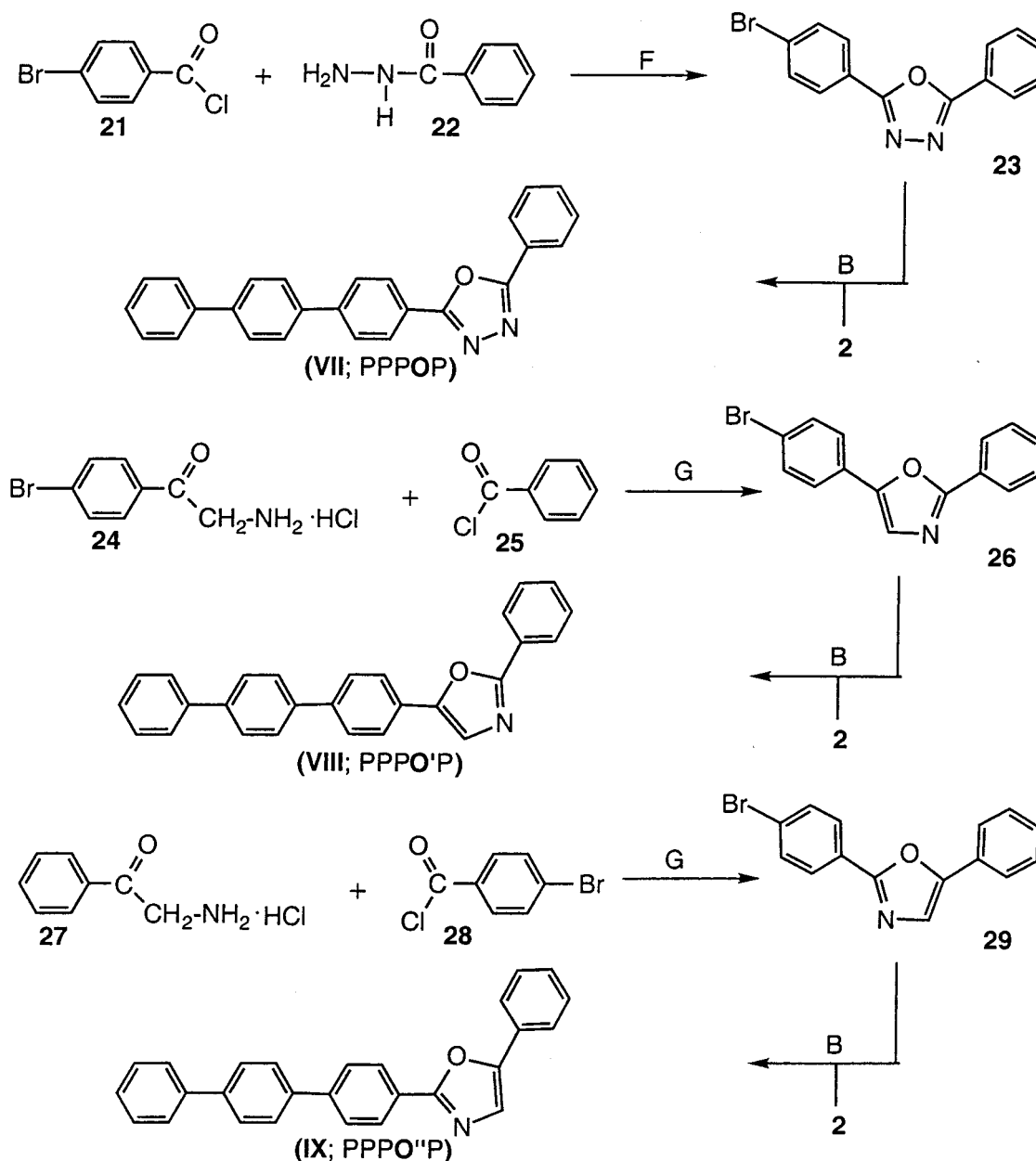

F (i) THF, NaHCO$_3$ (ii) Toluene, POCl$_3$
G (i) Pyridine (ii) POCl$_3$

destabilizes the mesophase. Although the thermal behavior of this compound has been reported before by Schubert and Sagitdinov, mesophase formation was not mentioned.[21] In our case, however, we detected a monotropic nematic phase upon cooling that was only stable over a small temperature range (313−322 °C).

Table 2 shows the DSC results of the hockey stick series wherein we rotate the substitution pattern in the thiophene moiety. This results in a major destabilization of the liquid crystalline state. In contrast with PPPTP (**III**), both PPPT′P (**V**) and PPPT″P (**VI**) show a monotropic nematic phase upon cooling that is stable over a one- or two-degree temperature range and is only apparent using optical microscopy. It is noteworthy that rotating the thiophene moiety—and thereby the direction of the dipole moment associated with the sulfur atom—barely affects the melting point. In an attempt to explain this dramatic loss of the mesophase stability we must factor in

the reduction of the excocyclic bond angle and the perturbation of conjugation. The exocyclic bond angle associated with 2,5-substituted thiophenes is 148°, and more "linear" then the 138° for the 3,5- and 2,4- analogues. However, this geometrical difference may be of less importance than the interruption of conjugation in the 3,5-and 2,4-isomers. This latter effect will be reflected in lower values of the electronic polarizability and will thereby reduce the anisotropy of the attractive interactions among PPPT′P and PPPT″P molecules relative to 2,5-substituted PPPTP.

The DSC results of the oxadiazole, PPPOP (**VII**), and oxazole, PPPO′P (**VIII**), and PPPO″P (**IX**) are summarized in Table 3. In this series of modified, hockey stick mesogens we were able to change the strength and direction of the electrostatic dipole moment while keeping the overall molecular shape unchanged. The oxadiazole derivative, PPPOP (**VII**), exhibits a remarkably low melting range (226−253 °C) compared to

SCHEME 9: The Synthetic Routes to the *m*-Phenylene-Modified *p*-Quinquephenyls (X and XI)
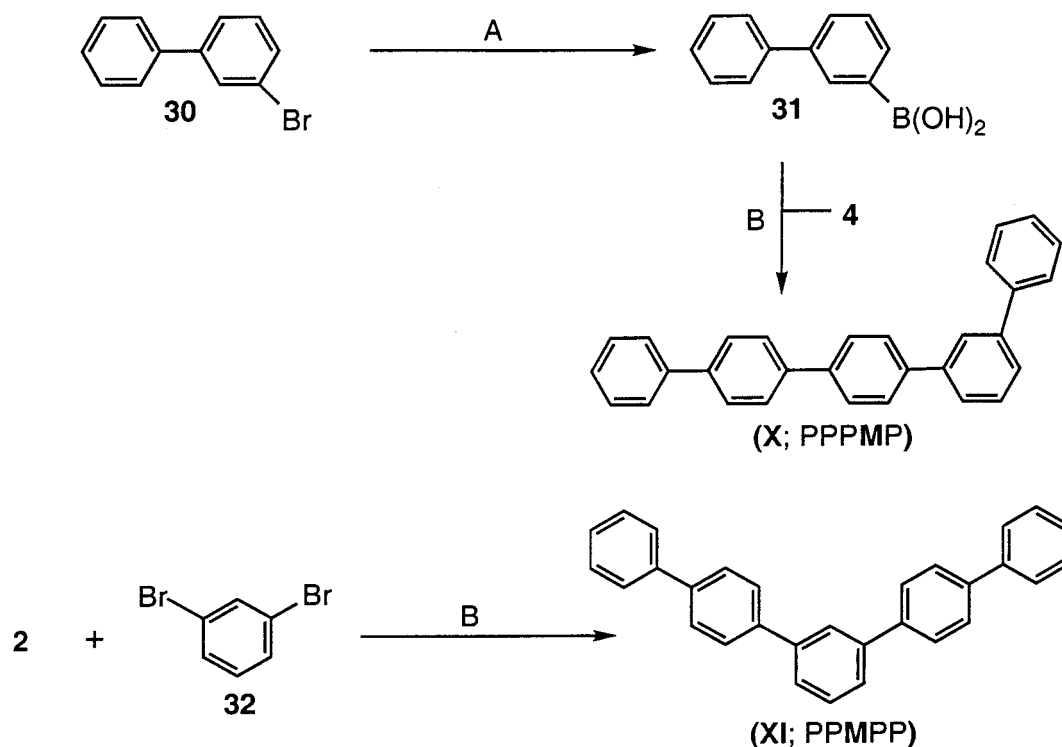
A (i) *n*-BuLi, THF (-78 °C); (ii) (MeO)$_3$B, THF (-78 °C); (iii) 10% HCl

B Pd(PPh$_3$)$_4$, 1,2-dimethoxyethane, 2M-Na$_2$CO$_3$

TABLE 1: Transition Temperatures (°C) and Enthalpies (KJ mol^{-1}) (in italics) for the 2,5-Thiophene-Modified *p*-Quinquephenyl Series. Second Heating and Cooling (10 °C min^{-1})

Compound	Phase behavior
(PPPPP; I)	K $\underset{380(-22)}{\overset{388(44)}{\rightleftarrows}}$ N $\underset{408(-0.9)}{\overset{420(0.7)}{\rightleftarrows}}$ I
(PPPPT; II)	K $\underset{371(-20)}{\overset{381(22)}{\rightleftarrows}}$ N $\underset{417(-0.6)}{\overset{425(0.7)}{\rightleftarrows}}$ I
(PPPTP; III)	K $\underset{288(-19)}{\overset{289(22)}{\rightleftarrows}}$ S$_A$ $\underset{315(-1)}{\overset{316(3)}{\rightleftarrows}}$ N $\underset{356(-0.2)}{\overset{356(0.5)}{\rightleftarrows}}$ I
(PPTPP; IV)	K $\underset{318(-36)}{\overset{322(39)}{\rightleftarrows}}$ N* $\underset{321(-0.2)}{\rightarrow}$ I

2-terphenyl-4-*yl*-5-phenyl thiophene (PPPTP)

Figure 1. The DSC trace of 2-terphenyl-4-*yl*-5-phenyl thiophene (PPPTP; **III**); second heating run (recorded at 10 °C min^{-1}).

the parent compound PPPPP (388−419 °C). Again both SmA and N phases could be observed although the thermal stability of the SmA is limited (a 2−3 °C range) and can only be observed on cooling with microscopy. The nematic phase, on the other hand, becomes more stabilized and has a window of almost 60 °C. Both of the oxazole hockey-stick mesogens show only a monotropic N phase upon cooling. For both isomers we found that the monotropic phase is very unstable and crystallization occurs rapidly. In these cases it is very unlikely that the difference in phase behavior and stability can be explained by geometry: The exocyclic bond angle associated with the 2,5-oxadiazole heterocycle is 136°, and 134° for both oxazole isomers. One prominent difference between PPPOP and the oxazole analogues is the magnitude of the dipole moments: ∼4 D in oxadiazole and ∼1.5 D in oxazole. Also, the oxadiazole
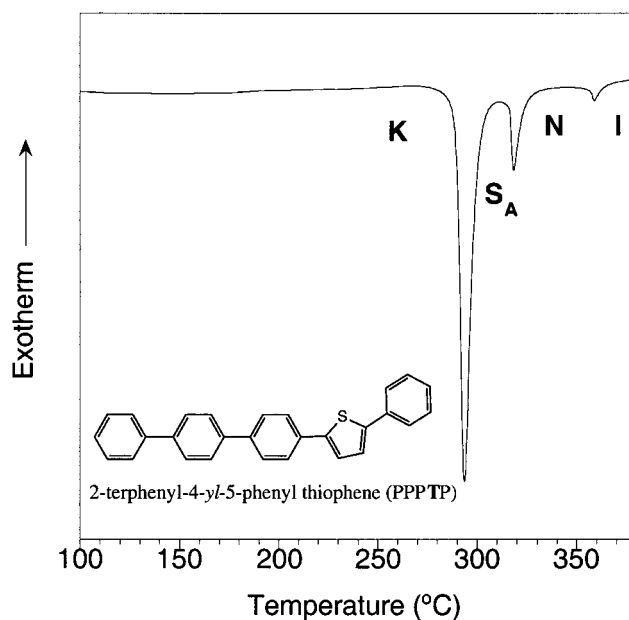
heterocycle allows conjugation through the molecule, while conjugation is impaired in both oxazole isomers.[10]

The DSC results of the final series of *m*-phenylene-modified quinquephenyls are summarized in Table 4. Here we have investigated the 1,3-phenylene analogues of the hockey stick, PPPMP (**X**), and boomerang, PPMPP (**XI**). Both compounds show no mesomorphic behavior on heating or cooling. In this case the 1,3-phenylene unit, with its 120° exocyclic bond angle, severely distorts the overall linear shape of PPPPP and exceeds

TABLE 2: Transition Temperatures (°C) and Enthalpies (KJ mol⁻¹) (in italics) for the Different Isomers of 2-Terphenyl-4-*yl*-5-phenyl Thiophene. Second Heating and Cooling (10 °C min⁻¹)
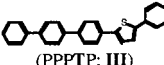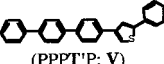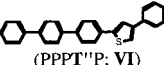
Compound	Phase behavior
(PPPTP; **III**)	$K \underset{288(-19)}{\overset{289(22)}{\rightleftarrows}} S_A \underset{315(-1)}{\overset{316(3)}{\rightleftarrows}} N \underset{356(-0.2)}{\overset{356(0.5)}{\rightleftarrows}} I$
(PPPT'P; **V**)	$K \underset{278}{\overset{288(43)}{\rightleftarrows}} N^* \underset{280}{\rightleftarrows} I$
(PPPT''P; **VI**)	$K \underset{275}{\overset{281(42)}{\rightleftarrows}} N^* \underset{277}{\rightleftarrows} I$

TABLE 3: Transition Temperatures (°C) and Enthalpies (KJ mol⁻¹) (in italics) for the Oxadiazole and Oxazole Hockey Sticks. Second Heating and Cooling (10 °C min⁻¹)
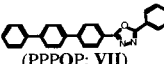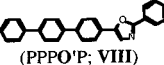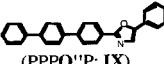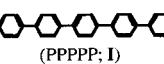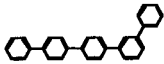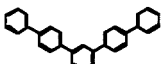
Compound	Phase behavior
(PPPOP; **VII**)	$K \underset{191}{\overset{226(41)}{\rightleftarrows}} S_A^* \underset{195}{\rightleftarrows} N \underset{343(-0.3)}{\overset{253(0.1)}{\rightleftarrows}} I$
(PPPO'P; **VIII**)	$K \underset{225}{\overset{231(42)}{\rightleftarrows}} N^* \underset{230}{\rightleftarrows} I$
(PPPO''P; **IX**)	$K \underset{183}{\overset{212(37)}{\rightleftarrows}} N^* \underset{195}{\rightleftarrows} I$

TABLE 4: Transition Temperatures (°C) and Enthalpies (KJ mol⁻¹) (in italics) for the 1,3-Phenylene-Modified *p*-Quinquephenyl Series. Second Heating and Cooling (10 °C min⁻¹)

Compound	Phase behavior
(PPPPP; **I**)	$K \underset{380(-22)}{\overset{388(44)}{\rightleftarrows}} N \underset{408(-0.9)}{\overset{420(0.7)}{\rightleftarrows}} I$
(PPPMP; **X**)	$K \underset{234(-54)}{\overset{258(56)}{\rightleftarrows}} I$
(PPMPP; **XI**)	$K \underset{257(-54)}{\overset{275(55)}{\rightleftarrows}} I$

the geometrical packing constraints required for calamitic mesogens. Concomitantly, the *meta* substitution disrupts the conjugation through the entire molecule.

We have summarized the phase behavior of the hockey stick and boomerang mesogens in Figures 2a and 2b. Both figures demonstrate clearly that introducing nonlinearity into the classic calamitic mesogen PPPPP results in a dramatic lowering of the transition temperatures that appears to scale with the exocyclic bond angle of the heterocycle. Also, when the exocyclic bond angle is reduced the LC phase is destabilized. The *m*-phenylene analogues PP**PMP** (**X**) and PP**MPP** (**XI**) are exceptions. These relatively high melting points are probably due to strong cohesion stemming from aromatic−aromatic packing interactions in the crystal lattice; we note that the crystal morphology of PP**MPP** (needles) is qualitatively different from the other PP**X**PP molecules (platelet flakes) and may be indicative of a different packing motif. The asymmetric hockey stick mesogens PP**PTP** (**III**) and PP**POP** (**VII**) show pronounced drops in
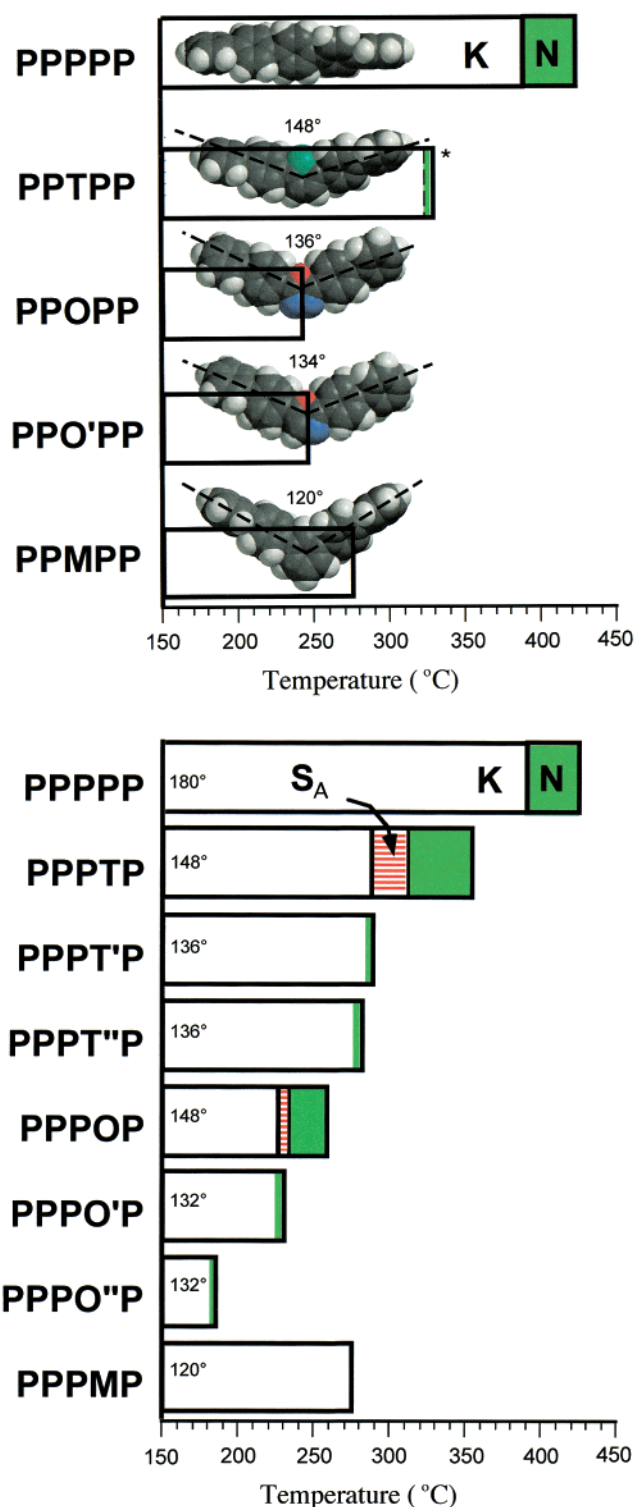
Figure 2. Summary of the thermal analysis data for hockey stick- and boomerang-shaped mesogens. (*) indicates that the phase behavior is monotropic and can be observed on cooling only. (K denotes crystal, S_A smectic-A, and N nematic phase, respectively.)

melting points and enhanced thermal ranges of liquid crystallinity that include both the N and SmA phases.

Optical Microscopy. The phase behavior of the compounds was characterized using polarizing microscopy. Samples were studied between untreated glass slides using heating and cooling rates of 5 °C/min. All of these mesophases exhibit very low viscosities and tend to form homeotropic, aligned monodomains. Most compounds (with the exception of PPPP**T**; **II**) are stable
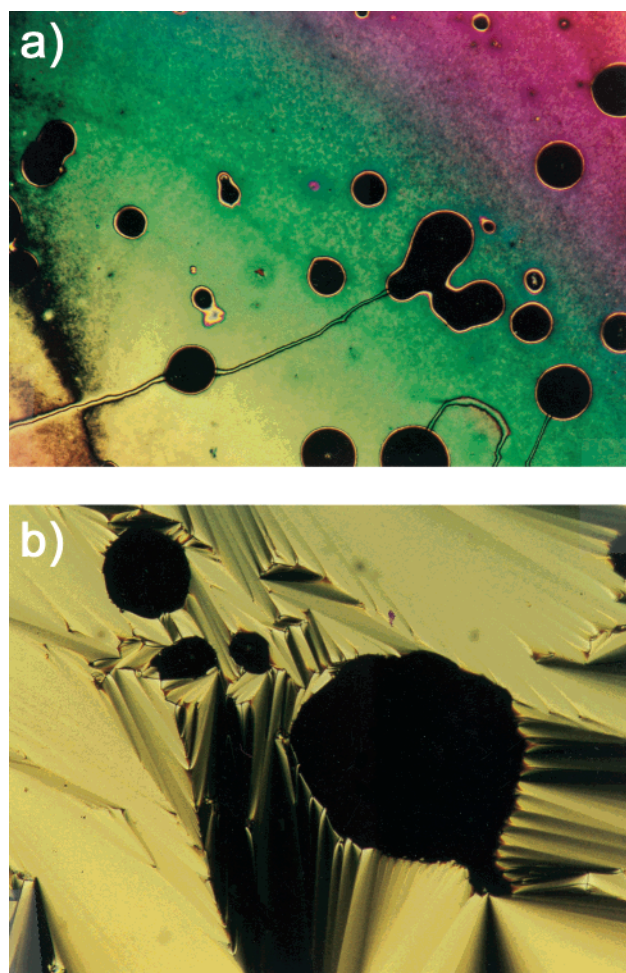
Figure 3. Microphotographs of the liquid crystalline phases of 2-terphenyl-4-*yl*-5-phenyl thiophene (PPPTP; **III**): (*a*) nematic phase (340 °C); (*b*) focal-conic texture of the smectic-A phase (315 °C).

in the melt and can be studied for prolonged periods of time. Some of the high-melting LCs (e.g., PPPPP) show a tendency to sublime.

As an example of classical calamitic texture formation in this class of molecules we show the textures of 2-terphenyl-4-*yl*-5-phenyl thiophene (PPPTP; **III**) in Figure 3. At 340 °C a characteristic nematic schlieren texture was observed (Figure 3a), and a typical focal-conic texture indicative of the SmA phase was observed at 315 °C (Figure 3b). Similar textures were observed for 2-terphenyl-4-*yl*-5-phenyl-1,3,4-oxadiazole (PP-P**O**P; **VII**).

X-ray Diffraction. *Crystal Structure of PP**T**PP and PP**O**PP.* We used single-crystal X-ray structure determinations in order to gain more detailed information about the molecular shape of these nonlinear mesogens, and to infer potential molecular packing motifs in the LC phases. Figure 4a and 4b show top (normal to the molecular face) and edge views of the molecular structure derived for the two boomerang-shaped mesogens, PP**T**PP and PP**O**PP.

Both molecules display "camber"—an ∼ 20° distortion of the boomerang's plane. It is also interesting to observe that the terminal phenyl rings in PP**O**PP are twisted out of the boomerang's plane as compared to PP**T**PP. This latter observation differs from reports by Baker et al. who studied the crystal structures of several *p*-phenylenes and found that in all cases the phenyl rings are coplanar.[22] With respect to the local geometry of the heterocycle, we found 2,5-exocyclic bond angles
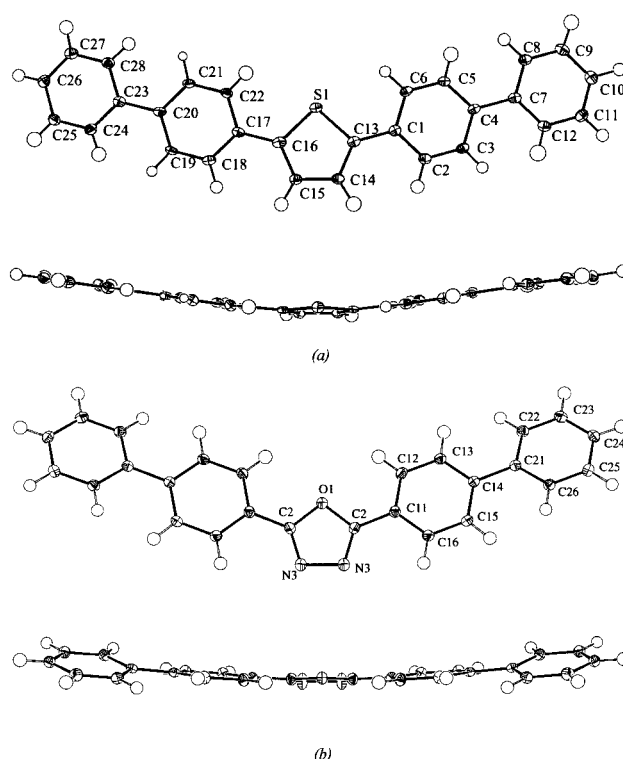

Figure 4. ORTEP diagrams of PP**T**PP (**IV**) and PP**O**PP (**VII**) with carbon ellipsoids drawn at the 50% probability level.
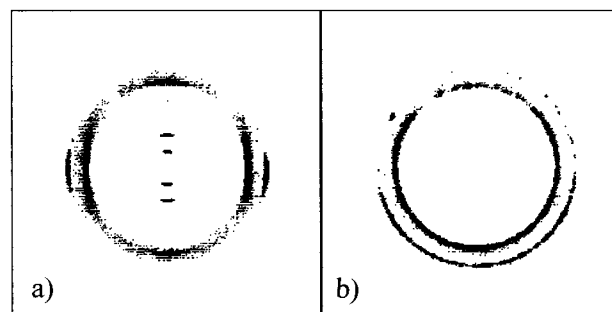
Figure 5. Diffraction patterns from the crystal phase of a single flake of PPPTP with the incident radiation oriented: (a) in the plane of the flake; (b) normal to the flake.

of 148.97° for PP**T**PP and 135.60° for PP**O**PP which is in close agreement with literature values.[6,8]

Molecular Packing in the Crystal and Mesophases of PPPTP. Figures 5a and b show uniaxial "fiberlike" diffraction patters obtained from the crystalline flakes of the hockey stick-shaped PPPTP mesogen. The flakes are an agglomeration of crystals that are aligned so that the (00*l*) planes are parallel to the surface of the flakes, but the crystals are randomly oriented about this surface normal. However, single crystals could be obtained when the samples were recrystallized from the melt. Diffraction patterns at various temperatures were obtained with incident X-rays along the edge of the flake. Examples of such data are shown in Figure 6. Despite the high degree of orientation in the 00*l* reflections, the *hk*0 reflections appear to be poorly oriented because of the intense off-equatorial reflections such as (021), (011), (012), etc.

The diffraction pattern in the crystalline phase could be indexed on an orthorhombic unit cell of dimensions a = 7.61 Å, *b* = 5.74 Å, and *c* = 43.5 Å. The packing of PPPTP appears to be similar to that of PP**T**PP as indicated by the similarity between the unit cell dimensions of the two structures; PPPTP

8854 *J. Phys. Chem. B, Vol. 105, No. 37, 2001*

Dingemans et al.

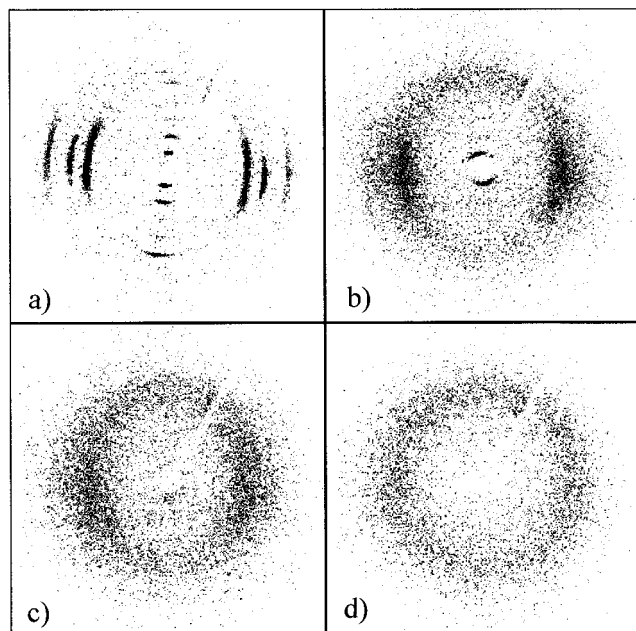**Figure 6.** The PPPTP single-crystal diffraction with the incident beam in the plane of the flake: (a) in its crystalline phase (245 °C); (b) in the Sm-A phase (292 °C); (c) in the nematic phase (350 °C); (d) in the isotropic phase (360 °C).

was calculated from the fiber-diffraction data and that of PPTPP calculated from single-crystal data. The series of reflections along the vertical (meridional) axis are indexed as 00*l* reflections, for *l*-even. Reflections up to *l* = 22 (*d* = 1.98 Å) were observed. Sometimes we also observed a 15 Å spacing (and weak evidence for a 30 Å one too) suggesting that there could be another polymorph of the phase that is analyzed in detail here. The three intense reflections along the horizontal (equatorial) axis could be indexed as 110, 020 (or 021), and 120 reflections. In the crystalline phase, during heating from ambient temperature to the crystal-smectic transition, the unit cell expands in an anisotropic way. The data show that the coefficient of thermal expansion of the *a*-axis is 40 × 10^{-6}/K and that of *b*-axis is 130 × 10^{-6}/K. Surprisingly, no comparable change in the *c*-axis dimensions was observed.

At about 290 °C the smectic phase appears with a layer spacing of 23.5 Å and a lateral intermolecular spacing of 4.8 Å. Upon further heating to about 315 °C the sample becomes nematic and the layer diffraction peak disappears leaving only diffraction corresponding to an intermolecular distance of 4.8 Å. Finally, at about 360 °C, the sample is isotropic with an average intermolecular distance of 4.5 Å.

A model for the packing of the molecules with accounts for the 43.5 Å *c*-axis dimension of the unit cell is given in Figure 7. In this model the hockey-stick PPPTP molecules pack end-to-end spanning the *c*-axis such that the layer spacing is approximately double that of the stick's handle-length (15 Å) plus the projection of the stick's "blade" on the direction of the handle (5.4 Å), i.e., 2 × 20.4 = 40.8 Å (Figure 7a). The dimensions along the *c*-axis collapse to ∼24 Å on entering the Sm-A phase. This is evidence that the hockey-stick handles interdigitate and yield a bilayerlike structure with a spacing slightly larger than the rectilinear PPPTP length (20.4 Å). The absence of any ambiguities in the length of the PPPTP mesogens gives a very clear picture of supramolecular packing of this nonlinear molecule in its Smectic-A phase.
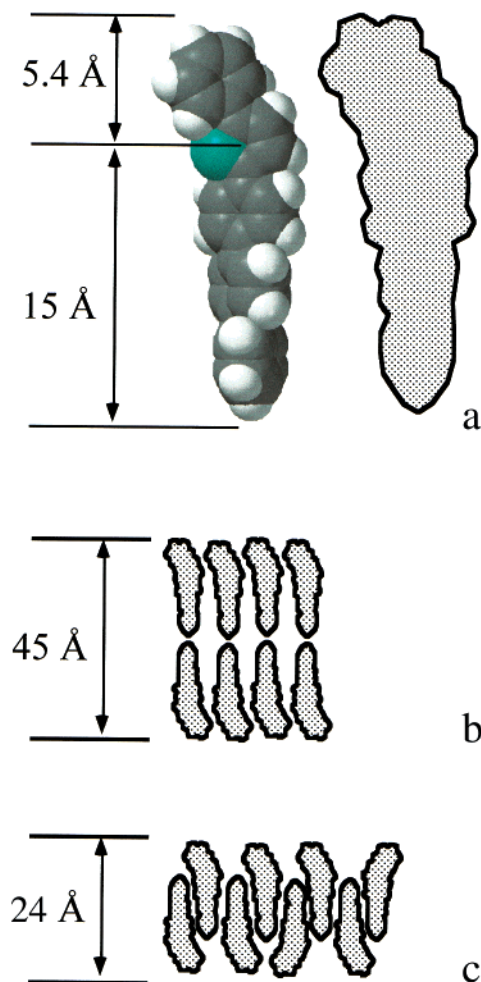

Figure 7. Molecular and supramolecular architectures for PPPTP (a) space filling model and schematic molecular outline; (b) the packing in the crystal; and (c) the interdigitated arrangement of the hockey stick-shaped mesogens in a Sm-A bilayerlike phase.

Discussion

The unusual electrooptic properties of liquid crystals is a consequence of long-range molecular orientational order in a fluid phase. To exploit these properties a more detailed understanding of structure−property relationships is needed. This is reinforced by recent unanticipated discoveries of ferroelectricity in nonlinear liquid crystals[23] and chiral supramolecular structures derived from achiral mesogens.[24] In recent years we have investigated a wide variety of nonlinear thermotropic liquid crystals (LCs) based on 2,5-substituted thiophenes.[25] One plausible and recurring finding is that nonlinear mesogens exhibit lower transition temperatures and appear to promote smectic phase formation. More recently we published results on nonlinear boomerang-shaped mesogens derived from esters of a symmetric oxadiazole mesogenic core; one such mesogen exhibited four distinct smectic mesophases.[26] However, the geometrical role of heterocycles in LC esters remains hard to quantify since other factors (such as the polar ester linkages that flank the heterocycle) may play a critical role in the stabilization of such mesophases. To exclude such factors we have synthesized simple calamitic liquid crystalline model compounds that are variations on *p*-quinquephenyl. Eleven model compounds were prepared using a standard Suzuki cross-coupling protocol. We found that this chemistry enabled us to successfully insert heterocyclic units such as thiophene, oxadiazole, and oxazole into a *p*-quinquephenyl molecular

framework. Such insertions allow us to control the overall mesogen shape, its conjugation, and the size and direction of the electrostatic dipole moment in the mesogenic core. For all compounds satisfactory yields were obtained, except for the coupling reactions that involved oxazole intermediates. These showed a rapid decomposition of the palladium catalyst and the desired compounds could only be isolated in small yields. The chemical structures of the final products were confirmed using high-resolution mass-spectroscopy (MS), elemental analysis, and infrared spectroscopy (IR).

In this study we've tried to identify generic characteristics of the resulting nonlinear mesogens and confirm trends we previously found.[25,26] On going from PPPPP to PPPTP to PPPOP, nonlinearity increases in the mesogenic core, and this depresses the melting point, T_{mp}, the crystal-to-fluid phase transition (Figure 5). For example, in PPPOP, T_{mp} is lowered by more than 150 °C below that of the parent mesogen PPPPP. With the exception of the *meta*-substituted quinquephenylenes PPPMP and PPMPP, the observed trends in T_{mp} seem to track the nonlinearity of the mesogens, i.e., packing considerations in the crystal dominate the solid-to-fluid transition. But perhaps more important, geometry appears to dictate the phase type: we discovered smectic phases in the nonlinear mesogens PPPTP and PPPOP. We were initially surprised to find that mesogen nonlinearity stabilizes a stratified smectic phase in this class of molecules as the quinquephenylenes do not contain flexible tails, heretofore thought to be prerequisite for smectic formation in low molar mass liquid crystals. However on further consideration of theoretical rationale for smectic-phase formation in ideal, rigid, rodlike mesogens[27] one can speculate why the nonlinearity of PPPTP—the geometrical "defect" associated with the nonlinear thiophene unit—stabilizes a smectic phase: In the nematic phase of PPPTP, the defect (nonlinear shape) should inhibit mesogen translation along the nematic director (longitudinal diffusion). On lowering the temperature, increased nematic order exaggerates the packing conflicts of this defect and its associated excluded volume. Dynamic packing conflicts can be ameliorated by stratification—condensing the defects into well-defined zones. In turn, this condensation redistributes excluded volume among *all* mesogens while facilitating lateral diffusion within smectic layers. Both are entropically favorable processes that more than compensate for the loss of longitudinal translational freedom accompanying the formation of smectic strata. Moreover, this explanation does not conflict with putative explanations of smectic formation in more conventional liquid crystals wherein layering is attributed to "nanophase separation" of the chemically distinct components of typical mesogens: the aromatic mesogenic cores are said to phase-separate from their aliphatic flexible tails when the latter exceed some critical length. That is because similar excluded volume interactions underlie smectic phase formation in these conventional mesogens. In fact, deuterium NMR observations suggested that mesogen tails experience more conformational freedom—demand less excluded volume and have higher entropy—on going from the nematic to the smectic architecture. In other words, partitioning the moderately chemically distinct components into mutually exclusive zones is not the driver but merely a byproduct of smectic phase formation.[28] Such entropic/excluded volume arguments certainly must apply to molecules such as PPPTP as this all-aromatic molecule is chemically uniform. Sexiphenyl is another example of a chemically uniform, smectic thermotropic liquid crystal without flexible alkyl chains.[17]

But what about the role of electrostatic interactions in this class of liquid crystals? Unfortunately even in this simple series

of substituted polyphenylenes, insertion of heterocyclic rings into the molecular framework does more than just alter the mesogen shape. Electric dipole moments, and perhaps more importantly electronic conjugation is perturbed. On a coarse level, the aromaticity and associated conjugation in PPPTP (and PPTPP) should be similar to the parent mesogen PPPPP if one infers aromaticity from heats of combustion; benzene and thiophene are quite similar (152 and 121 kJ/mol, respectively).[29] But there are more subtle indicators of changes in electronic attributes of these mesogens: the wavelength of maximum UV absorption, λ_{max}, shifts to higher values in the UV spectra of the series PPPPP, PPPPT, PPPTP, and PPTPP.[30] Similar perturbations come into play when the thiophene heterocycle is "rotated" in PPPTP. This is even evident upon visual inspection of the crystals (the 2,5 isomer PPPTP is yellow while the 3,5- and 2,4- isomers, PPPT′P and PPPT″P, are colorless). While it is difficult to quantify the changes in the electrostatic profiles of the different quinquephenylene-based mesogens, significant changes in the anisotropy of the molecular polarizibility should impact mesomorphism according to the Maier-Saupe model of the origins of liquid crystallinity.[31] In fact, if you look at our results at "low resolution," the role of polarizability/conjugation is apparent. For example, the melting points of all of the hockey stick-shaped molecules fall into roughly two classes: the thiophenes with $T_{mp} \approx 285$ °C, and the diazole and oxazoles with $T_{mp} \approx 220$ °C. Yet only one member of each class exhibits enantiotropic mesomorphism, the 2,5-thiophene derivative PPPTP and the oxadiazole derivative PPOPP. The other hockey stick molecules, the 3,5- and the 2,4-thiophenes (PPPT′P and PPPT″P) and the two oxazoles (PPPO′P and PPPO″P), only exhibit very small monotropic mesophases. Since conjugation is clearly perturbed in these latter four mesogens relative to PPPTP and PPPOP, electrostatic interactions must play a role in stabilizing the mesophase for these nonlinear liquid crystals. However, the order of magnitude difference in the dipole moments between PPPTP and PPPOP, 0.47 and 4.0 D, respectively, in conjunction with the similarity of their mesophases (smectic-A phase followed by a nematic) suggests that dipole—dipole interactions are not dominant. Rather, anisotropic attractive interactions stemming form subtle aspects of the molecular polarizability probably govern the mesophase stability observed in nonlinear mesogens.

Concluding Remarks

In summary, molecular geometry is an important variable in the reported series of nonlinear, all-aromatic liquid crystals influencing the melting temperature of the crystals but mesophase type and range may be governed by attractive electrostatic interactions. The unanticipated discovery of smectic-A phases in hockey stick-shaped molecules PPPTP and PPPOP emphasize the role of molecular geometry. X-ray studies of PPPTP show an interdigitated supramolecular arrangement of molecules in the smectic phase. The observations of both nematic and smectic architectures in this comparatively simple class of liquid crystals should encourage further studies of the origins of liquid crystallinity, in particular studies using computer simulations. We anticipate that in simulations the polyphenylenes may be represented by a limited number of multisite interactions,[32] enabling a more quantitative understanding of thermotropic mesomorphism in terms of electrostatic and excluded volume interactions.

Experimental Details

General. Tetrahydrofuran (THF) and diethyl ether were dried over and distilled from sodium/benzophenone prior to use.

Reagents were purchased from commercial sources and were used without further purification. 2,5-Bisbiphenyl-4-*yl*-1,3,4-oxadiazole (PP**O**PP) and 2,5-bisbiphenyl-4-*yl*-oxazole (PP**O′**PP) were purchased from Aldrich Chemical Co. Tetrakis(triphenylphosphine)palladium(0) was synthesized according to literature procedures.[33] The structures of intermediates were confirmed by ^{1}H NMR (Bruker WM250, 250 MHz) and ^{13}C NMR (Varian Gemini 2000-300, 75.46 MHz). Reactions were monitored by thin-layer chromatography using an eluent of hexane/ethyl acetate (9/1). Gas chromatograms (GC) were obtained with a Hewlett-Packard 5890 gas chromatograph equipped with a 30 m, nonpolar, HP-5MS column. Mass spectra (MS) were obtained using a Hewlett-Packard 5972 spectrometer; M+ represents the molecular ion. Infrared spectra were obtained with a Bio-rad FTS-7 spectrometer. Transition temperatures were determined by using a Seiko DSC 120 differential scanning calorimeter, calibrated with indium (99.99%) (mp = 156.5 °C, ΔH = 28.315 J/g) and tin (99.99%) (mp = 232.0 °C, ΔH = 54.824 J/g). The second heating (10 °C min^{-1}) as well as the cooling scans (10 °C min^{-1}) were recorded. To prevent the LCs from subliming out of the sample pans we used high-pressure DSC sample capsules (Seiko, AL 15). Mesophases were identified with a Nikon Microphot-FX polarizing microscope equipped with a linkam hotstage. All products (with the exception of **VII**−**IX**) were analyzed at the North Carolina State University Mass Spectroscopy Facility, using a JEOL (Tokyo Japan) HX110HF mass spectrometer. The resolving power of the mass spectrometer was 10 000, the accelerating voltage 10 keV, and the ion source temperature 160 °C. The oxadiazole- and oxazole-based liquid crystals (**VII**−**IX**) were soluble in chloroform and could therefore be analyzed using a Waters Integrity MS system.

X-ray Diffraction. Single-crystal data were collected on a Siemens SMART diffractometer, using the omega scan mode (Mo Kα λ = 0.71073 Å). Direct methods revealed all of the non-hydrogen atoms for compounds PP**T**PP (**IV**) and PP**O**PP. All non-hydrogen atoms were refined anisotropically for compounds PP**T**PP (**IV**) and PP**O**PP, and the final least-squares refinement for each structure converged at the *R*-factors reported in Table 5. All calculations were performed using NRCVAX software.[34] Full crystallographic details for the compounds PP**T**PP (**IV**) and PP**O**PP have been provided in the Supporting Information.

Supramolecular structural data were collected in three different modes. First, a few thin, platelike, multi-crystal flakes of PPP**T**P were spread out on a single-crystal holder, and 1-D scans were collected in reflection geometry on a Philips powder diffractometer. The platelike morphology primarily exhibit the layer-line (00*l*) reflections in these scans. Therefore, most of the data were collected in transmission geometry. Several thin flakes were sealed in a quartz capillary and 1-D data were collected on an Inel detector. The most easily interpretable data were obtained by sealing a single flake in a capillary and collecting 2-D diffraction data on a Bruker area detector. Data were collected using Cu Kα radiation using an incident beam monochromator. The sample was heated with a nitrogen stream, and the temperature was measured using a thermocouple located near the sample.

Synthesis of Precursors. *4-Biphenylboronic acid* (**2**). To a cooled solution (−78 °C) of 4-bromobiphenyl (**1**) (9.32 g, 0.04 mol) in 100 mL dry THF, was added dropwise, 16 mL of a 2.5 M solution of *n*-BuLi in hexanes. This mixture was stirred and kept at −78 °C for 2.5 h. A solution of trimethyl borate (8.31 g, 0.08 mol) was slowly added over 30 min after which the

TABLE 5: Crystal Data and Structure Refinement for PP T PP (IV) and PP O PP

	PP**T**PP (**IV**)	PP**O**PP
empirical formula	$C_{28}H_{20}S$	$C_{26}H_{18}N_2O$
formula weight	388.52	374.44
temperature (K)	198	198
crystal system	monoclinic	orthorhombic
color of crystal	yellow	colorless
space group	$P\,2_1/n$	P nam
unit cell dimensions		
a (Å)	7.4972(4)	6.1807(3)
b (Å)	5.7929(3)	7.1839(4)
c (Å)	43.6290(21)	41.5379(20)
β (deg)	93.3420(10)	-
volume (Å^3)	1891.61	1844.35
Z	4	4
F(000)	816.87	784.43
crystal size (mm)	$0.40 \times 0.20 \times 0.01$	$0.25 \times 0.25 \times 0.05$
θ range for data collection (deg)	3 to 50	3 to 60
limiting indices		
	$-8 \leq h \leq 8$	$0 \leq h \leq 8$
	$0 \leq k \leq 6$	$0 \leq k \leq 10$
	$0 \leq l \leq 51$	$0 \leq l \leq 57$
reflections collected	10237	19766
independent reflections	3317	2718
refinement method	full matrix least-squares	full matrix least-squares
data/restraints/parameters		
goodness of fit	2.20	2.10
R1	0.062	0.045
wR2	0.069	0.047
R indices (all data)		
R1	0.100	0.070
wR2	0.098	0.049

reaction mixture was allowed to warm up to room temperature overnight. The resulting mixture was acidified with 60 mL of a 10% HCl solution and stirred for 1 h at room temperature. The crude product was extracted into diethyl ether (3 × 100 mL), and washed successively with a concentrated sodium carbonate solution and water. The ether was removed by distillation and the crude product was recrystallized twice from a water/ethanol mixture (95/5). The off-white crystals were dried under vacuum overnight at 60 °C to obtain 6.8 g (86%) of 4-biphenylboronic acid. ^{1}H NMR (250 MHz, Acetone-d_6) δ 7.25 (s, 2H, −B(OH)$_2$), 7.35 (t, J = 7 Hz, 1H, ArH), 7.45 (t, J = 7 Hz, 2H, ArH), 7.65 (d, J = 8 Hz, 2H, ArH), 7.68 (d, J = 8 Hz, 2H, ArH), 7.98 (d, J = 8 Hz, 2H, ArH). ^{13}C NMR (75.46 MHz, Acetone-d_6): δ 126, 127, 127.5, 128.9, 134.8, 134.9, 140.9, 142.7.

4-Bromo-p-terphenyl (**4**). A 200 mL two-neck flask equipped with magnetic stir bar, reflux condenser, and argon inlet was charged (under argon atmosphere) with 1-bromo-4-iodobenzene (**3**) (4.1 g, 14.5 mmol) and 5 mol % tetrakis(triphenylphosphine)palladium(0) (0.8 g, 0.7 mmol). A volume of 80 mL of dimethoxyethane (DME) was added and this yellow solution was stirred for 10 min at room temperature. 4-Biphenylboronic acid (**2**) (2.97 g, 15 mmol) and 80 mL of 2 M Na$_2$CO$_3$ were added, and this mixture was refluxed under argon atmosphere for 12 h. After cooling to room temperature the mixture was extracted with dichloromethane (2 × 100 mL) and the organic layer was washed with water and dried over MgSO$_4$. After removal of the MgSO$_4$ by filtration, the solution was filtered over a small pad of silica gel and Celite. The solvent was removed by distillation and the crude 4-bromo-*p*-terphenyl was recrystallized twice from dichloromethane to obtain 3.6 g (80%) of the title compound. GC: t_r = 11.7 min, (>99.9%), MS (*m/z*): 308/310 (M+), 228, 202, 152, 113. ^{1}H NMR (250 MHz, CDCl$_3$) δ 7.31−7.7 (m, 13 H, ArH). ^{13}C NMR (75.46 MHz,

CDCl$_3$) δ 138.86 (C-1), 128.62 (C-2), 131.94 (C-3), 121.62 (C-4), 139.61 (C-1′), 127.65 (C-2′), 127.49 (C-3′), 140.53 (C-4′), 140.53 (C-1″), 127.06 (C-2″), 128.88 (C-3″), 127.30 (C-4″).[35]

2-(4-Phenylboronic acid) thiophene (**8**). A 100 mL two-neck flask equipped with magnetic stir bar, reflux condenser, and argon inlet was charged (under argon atmosphere) with 1-bromo-4-iodobenzene (**3**) (1.13 g, 4 mmol) and 5 mol % tetrakis(triphenylphosphine)palladium(0) (0.23 g, 0.2 mmol). A volume of 30 mL of dimethoxyethane (DME) was added and this yellow solution was stirred for 10 min at room temperature. 2-Thiopheneboronic acid (**6**) (0.64 g, 5 mmol) and 30 mL of 2 M Na$_2$CO$_3$ were added and this mixture was refluxed under argon atmosphere for 12 h. After cooling to room temperature the mixture was extracted with diethyl ether (2 × 100 mL) and the organic layer was washed with water and dried over MgSO$_4$. The solvent was removed by distillation and the resulting crude product was twice recrystallized from EtOH to obtain 0.65 g (68%) 2-(4-bromophenyl) thiophene (**7**) as slight yellow platelets. The purity of the product was checked by TLC, one spot (silica gel, t_r = 0.65). GC: t_r = 7.85 min, MS (*m/z*): 238/240 (M+), 193, 158, 115. ^{1}H NMR (250 MHz, CDCl$_3$) δ 7.0−7.1 (m, 1H), 7.2−7.3 (m, 2H), 7.45 (dd, *J* = 7 Hz, 4H, ArH); ^{13}C NMR (75.46 MHz, CDCl$_3$) δ 121.5, 123.7, 125.5, 127.6, 128.4, 132.1, 133.6, 143.3.

2-(4-Bromophenyl) thiophene (**7**) 0.34 g, 14 mmol) was treated with magnesium (0.04 g, 16 mmol) in 10 mL of dry tetrahydrofuran (THF) under argon. After the initial reaction subsided the mixture was refluxed for 6 h and cooled to room temperature. This Grignard solution was added dropwise to a cooled (−78 °C) trimethyl borate solution (0.29 g, 28 mmol in THF 5 mL) and was allowed to warm up overnight. The resulting mixture was acidified with 10 mL of a 10% HCl solution and stirred for 1 h at room temperature. The crude product was extracted into diethyl ether (3 × 50 mL), washed successively with a concentrated sodium carbonate solution, and water. The ether was removed by distillation and the crude 2-(4-phenylboronic acid) thiophene (**8**) was recrystallized twice from water/ethanol (95/5) and used immediately. Yield: 0.14 g (48%).

2-Phenyl-5-thiopheneboronic acid (**12**). A 100 mL two-neck flask equipped with magnetic stir bar, reflux condenser, and argon inlet was charged (under argon atmosphere) with 2-bromothiophene (**9**) (4.08 g, 25 mmol) and 5 mol % tetrakis(triphenylphosphine)palladium(0) (1.44 g, 1.25 mmol). A volume of 30 mL of dimethoxyethane (DME) was added and this yellow solution was stirred for 10 min at room temperature. Phenylboronic acid (**10**) (3.41 g, 28 mmol) and 30 mL of 2 M Na$_2$CO$_3$ were added and this mixture was refluxed under argon atmosphere for 24 h. After cooling to room temperature the mixture was extracted with diethyl ether (3 × 100 mL) and the organic layer was washed with water and dried over MgSO$_4$. The solvent was removed by distillation and the resulting crude product was chromatographed over silica gel eluted with *n*-hexane/ethyl acetate (9:1) followed by recrystallization from EtOH to obtain 3.64 g (91%) 2-phenylthiophene (**11**) as slight yellow platelets. The purity of the product was checked by TLC, one spot (silica gel, t$_r$ = 0.55). GC: t_r = 6.07 min, MS (*m/z*): 160 (M+), 128, 115. ^{1}H NMR (250 MHz, Acetone-*d$_6$*) δ 7.11 (dd, *J* = 4 Hz, 1H), 7.29 (t, *J* = 8 Hz, 1H), 7.36−7.46 (m, 4H), 7.66 (d, *J* = 7 Hz, 2H); ^{13}C NMR (75.46 MHz, Acetone-*d$_6$*) δ 124.3, 126, 126.5, 128.4, 129.2, 129.9, 135.3, 144.9.

2-Phenylthiophene (**11**) (0.51 g, 3.2 mmol) in 10 mL of dry THF under argon atmosphere was cooled to 0 °C and 2 mL of 1.6 M *n*-BuLi in THF (3.2 mmol) was added over 10 min. The ice-bath was removed and the solution was refluxed for 20 min and allowed to cool to room temperature. The deep red solution

was slowly cannulated into a vigorously stirred solution of trimethyl borate (0.65 g, 6.4 mmol) in 5 mL of dry THF at −78 °C. The mixture was allowed to warm up to room temperature overnight, acidified with 10% HC, and stirred for 1 h. The aqueous mixture was extracted with diethyl ether (3 × 100 mL) and the organic layer was washed with water and dried over MgSO$_4$. The solvent was removed by distillation and the resulting crude product was recrystallized twice from water/ethanol (95/5). Yield was 0.45 g (69%) of 2-phenyl-5-thiopheneboronic acid (**12**). ^{1}H NMR (250 MHz, Acetone-*d$_6$*) δ 7.25−7.50 (m, 5H), 7.64−7.74 (m, 3H). ^{13}C NMR (75.46 MHz, Acetone-*d$_6$*) δ 105.9, 113.5, 125.4, 126.7, 126.8, 128.7, 130, 137.9.

2-Phenyl-4-thiopheneboronic acid (**16**). A solution of 2,4-dibromothiophene (**14**) (10 g, 41 mmol) in 10 mL of dry ether was added to a stirred solution of 16 mL of 2.5 M *n*-BuLi in hexanes, in 40 mL of dry ether at −70 °C. This solution was stirred under argon for several minutes and cyclohexanone (4.22 g, 43 mmol) in 5 mL of dry ethyl ether was added. The mixture was then allowed to warm to room temperature overnight and hydrolyzed with 20 mL of HCl (6 N). The dark orange solution was extracted with ethyl ether (2 × 100 mL) and the organic layer was successively washed with concentrated sodium carbonate, water, and dried over MgSO$_4$. The solvent was removed by distillation and the resulting orange oil was purified by vacuum distillation. 6.6 g (67%) of 4-bromo-2-(1-cyclohexenyl) thiophene was collected as a clear oil; bp 90−94 °C, 0.1 mmHg. GC: t_r = 8.07 min, MS (*m/z*): 242/244 (M+), 229, 216, 163, 135.

4-Bromo-2-(1-cyclohexenyl) thiophene (5.4 g, 22 mmol) was aromatized with dichlorodicyanoquinone (10 g, 43 mmol) in 65 mL benzene under argon atmosphere. The solution was stirred at room temperature for 30 min. After the initial exothermic reaction subsided the solution was refluxed for 5 h. After cooling to room temperature, the precipitate was filtered off and washed with 15 mL benzene. The combined organic layers were washed with 2N−NaOH until no more precipitate could be detected in the aqueous layer. The organic layer was washed with 5% HCl and dried over MgSO$_4$. Benzene was removed by distillation and the yellow crude product was dissolved in 250 mL hot hexane and filtered over a short alumina column. After removal of the hexane a white solid product was obtained which was recrystallized twice from ethanol to obtain 4.15 g (79%) of 4-bromo-2-phenyl thiophene (**15**). GC: t_r = 7.66 min, MS (*m/z*): 238/240 (M+), 159, 115. ^{1}H NMR (250 MHz, Acetone-*d$_6$*) δ 7.32−7.47 (m, 4H), 7.49 (d, *J* = 2 Hz, 1H), 7.67 (dd, *J* = 7 Hz, 2H). ^{13}C NMR (75.46 MHz, Acetone-*d$_6$*) δ 110.9, 123.3, 123.4, 126.4, 129.2, 129.9, 133.8, 146.2.

4-Bromo-2-phenyl thiophene (**15**) (2.1 g, 9 mmol) was treated with magnesium (0.24 g, 9.8 mmol) in 20 mL dry tetrahydrofuran (THF) under argon. After the initial reaction subsided the mixture was refluxed for 7 h. and cooled to room temperature. This Grignard solution was added dropwize to a cooled (−78 °C) trimethyl borate solution (1.9 g, 18 mmol in THF 10 mL) and was allowed to warm up to room temperature overnight. The resulting mixture was acidified with 20 mL of a 10% HCl solution and stirred for 2 h at room temperature. The crude product was extracted into diethyl ether (3 × 100 mL), washed successively with concentrated sodium carbonate solution, and water. The ether was removed by distillation and the crude 2-phenyl-4-thiopheneboronic acid (**16**) was recrystallized twice from water/ethanol (95/5). Yield: 0.45 g (25%). ^{1}H NMR (250 MHz, DMSO-*d$_6$*) δ 7.27 (t, *J* = 7 Hz, 1H), 7.40 (t, *J* = 8 Hz, 2H), 7.60 (d, *J* = 7 Hz, 2H), 7.74 (s, 1H), 7.94 (s, 1H), 8.09 (b,

−B(OH)$_2$); ^{13}C NMR (75.46 MHz, DMSO-d_6) δ 125.4, 127.5, 128.8, 128.9, 129.2, 134, 134.8, 143.

4-Phenyl-2-thiopheneboronic acid (**20**). A 200 mL two-neck flask equipped with magnetic stir bar, reflux condenser, and argon inlet was charged (under argon atmosphere) with 3-bromothiophene (**17**) (13 g, 80 mmol) and 5 mol % tetrakis(triphenylphosphine)palladium(0) (4.6 g, 4 mmol). A volume of 90 mL of dimethoxyethane (DME) was added and this yellow solution was stirred for 10 min at room temperature. Phenylboronic acid (**10**) (11 g, 90 mmol) and 90 mL of 2 M Na$_2$CO$_3$ were added and this mixture was refluxed under argon atmosphere for 24 h. After cooling to room temperature the mixture was extracted with diethyl ether (3 × 200 mL) and the organic layer was washed with water and dried over MgSO$_4$. The solvent was removed by distillation and the resulting crude product was chromatographed over Celite eluted with hot ethanol, followed by recrystallization from EtOH to obtain 8.2 g (64%) of 3-phenyl thiophene (**18**) as colorless crystals. GC: t_r = 6.05 min, MS (*m/z*): 160 (M+).

Bromine (5.0 g, 32 mmol) in 50 mL of glacial acetic acid was added dropwise to a solution of 3-phenyl thiophene (**18**) (5.0 g, 32 mmol) in 65 mL of glacial acetic acid and the resulting yellow solution was refluxed for 5 h and cooled to room temperature. The reaction mixture was diluted with 300 mL of water and extracted with ethyl ether (2 × 100 mL). The combined organic layers were washed with concentrated sodium carbonate, and dried over MgSO$_4$. The solvent was removed by distillation and the crude product was chromatographed over a short silica gel column with hexane/ethyl acetate (90/10) as eluent. After removing the solvent by distillation, a slight yellow product was obtained which was recrystallized twice from ethanol. Yield; 5.5 g (73%) of 2-bromo-4-phenyl thiophene (**19**). GC: t_r = 7.56 min, MS (*m/z*): 238/240 (M+), 158, 115, 79. ^{1}H NMR (250 MHz, Acetone-d_6) δ 7.31 (t, J = 7 Hz, 1H), 7.40 (t, J = 7 Hz, 2H), 7.56 (d, J = 2 Hz, 1H), 7.64−7.72 (m, 3H); ^{13}C NMR (75.46 MHz, Acetone-d_6) δ 112.8, 122.6, 122.7, 126.5, 128.1, 129.5, 135.2, 143.2.

2-Bromo-4-phenyl thiophene (**19**) (1.05 g, 4.4 mmol) was treated with magnesium (0.12 g, 4.9 mmol) in 10 mL of dry tetrahydrofuran (THF) under argon. After the initial reaction subsided the mixture was refluxed for 7 h and cooled to room temperature. This Grignard solution was added dropwise to a cooled (−78 °C) trimethyl borate solution (1.0 g, 9 mmol in THF 5 mL) and was allowed to warm up to room temperature overnight. The resulting mixture was acidified with 10 mL of a 10% HCl solution and stirred for 2 h at room temperature. The crude product was extracted into diethyl ether (3 × 50 mL), and washed successively with concentrated sodium carbonate solution and water. The ether was removed by distillation and the crude 4-phenyl-2-thiopheneboronic acid (**20**) was recrystallized twice from water/ethanol (95/5) and used immediately. Yield: 0.66 g (73%).

2-(4-Bromophenyl)-5-phenyl-1,3,4-oxadiazole (**23**). To a stirred solution of benzoic hydrazide (**22**) (3.1 g, 23 mmol) and sodium bicarbonate (1.93 g, 23 mmol) in 40 mL of water was added a solution of 4-bromobenzoyl chloride (**21**) (5.05 g, 23 mmol) in 30 mL of THF. After 30 min, the solids were filtered, washed with water, and dried overnight (vacuum at 40 °C).

A solution of the amide (7 g, 22 mmol) in 80 mL of dry toluene with 40 mL of POCl$_3$ was refluxed for 6 h. Toluene and excess POCl$_3$ were removed by vacuum distillation and the resulting product was washed, dried, and recrystallized from ethanol. Yield: 6.2 g (90%) of 2-(4-bromophenyl)-5-phenyl-1,3,4-oxadiazole (**23**). GC: t_r = 13.91 min, MS (*m/z*): 300/

302 (M+), 183, 165, 105, 77. ^{1}H NMR (250 MHz, CD$_2$Cl$_2$) δ: 7.52−6.60 (m, 3H), 7.70 (d, J = 8 Hz, 2H), 8.01 (d, J = 8 Hz, 2H), 8.09−8.15 (m, 2H); ^{13}C NMR (75.46 MHz, CD$_2$Cl$_2$) δ: 123.3, 124.2, 126.5, 127.2, 128.6, 129.5, 132.2, 132.8, 164.2, 165.1.

2-Phenyl-5-(4-bromophenyl)-5-oxazole (**26**). To a stirred solution of benzoyl chloride (**25**) (4.22 g, 30 mmol) in 60 mL of dry pyridine was added 2-amino-4′-bromoacetophenone hydrochloride (**24**) (7.52 g, 30 mmol). This mixture was stirred for 30 min at room temperature and refluxed for 30 min. After cooling the reaction mixture, water was added and the precipitate was collected by filtration. The yellow solids were washed with excess water and dried. Yield: 7.9 g (83%). The amide intermediate (7.9 g, 25 mmol) was dissolved in 75 mL of POCl$_3$ and this solution was refluxed for 12 h. Most of the POCl$_3$ was removed by distillation and the remaining solution was slowly poured in 200 mL of ice water. The solids were collected by filtration, dried, and recrystallized from ethanol. Yield: 6.1 g (82%) of 2-phenyl-5-(4-bromophenyl)-5-oxazole (**26**). GC: t_r = 13.51 min, MS (*m/z*): 301 (M+), 165, 116, 89, 63. ^{1}H NMR (250 MHz, CDCl$_3$) δ 7.46 (t, J = 8 Hz, 1H), 7.56−7.64 (m, 3H), 7.83 (d, J = 7 Hz, 2H), 7.96 (d, J = 7 Hz, 2H), 8.12 (d, J = 8 Hz, 2H); ^{13}C NMR (75.46 MHz, CDCl$_3$) δ: 122.2, 123.9, 125.5, 126.3, 126.8, 127.1, 128.8, 130.5, 132.1, 150.2, 161.3.

2-(4-Bromophenyl)-5-phenyl-oxazole (**29**). To a stirred solution of 4-bromobenzoyl chloride (**28**) (2.6 g, 12 mmol) in 30 mL of dry pyridine was added 2-aminoacetophenone hydrochloride (**27**) (2.0 g, 12 mmol). This mixture was stirred for 30 min at room temperature and refluxed for 30 min. After cooling the reaction mixture, water was added and the precipitate was collected by filtration. The yellow solids were washed with excess water and dried. Yield: 3.69 g (97%). The amide intermediate (2.0 g, 6.3 mmol) was dissolved in 75 mL of POCl$_3$ and this solution was refluxed for 12 h. Most of the POCl$_3$ was removed by distillation and the remaining solution was slowly poured in 200 mL of ice water. The solids were collected by filtration, dried, and recrystallized from toluene. Yield: 1.5 g (79%) of 2-(4-bromophenyl)-5-phenyl-oxazole (**29**). GC: t_r = 13.25 min, MS (*m/z*): 301 (M+), 165, 77. ^{1}H NMR (250 MHz, CDCl$_3$) δ 7.33 (t, J = 7 Hz, 1H), 6.39−7.45 (m, 3H), 7.58 (d, J = 8 Hz, 2H), 7.68 (d, J = 8 Hz, 2H), 7.94 (d, J = 8 Hz, 2H); ^{13}C NMR (75.46 MHz, CDCl$_3$) δ 123.6, 124.3, 124.8, 126.4, 127.7, 127.8, 128.7, 129, 132.1, 151.6, 160.3.

3-Biphenylboronic acid (**31**). 3-Bromobiphenyl (**30**) (3.12 g, 13 mmol) in 30 mL of dry THF was treated with 5.33 mL of a 2.5 M n-BuLi solution in hexanes at −78 °C under argon and was kept at this temperature for 2 h. A solution of trimethyl borate (2.77 g, 26 mmol) in 20 mL of dry THF was added dropwise over 30 min. This mixture was allowed to warm up to room temperature overnight. The resulting mixture was acidified with 20 mL of a 10% HCl solution and stirred for 2 h at room temperature. The crude product was extracted into diethyl ether (3 × 100 mL) and washed successively with concentrated sodium carbonate solution and water. The ether was removed by distillation and the crude 3-biphenylboronic acid (**31**) was recrystallized twice from water/ethanol (95/5). Yield: 1.98 g (75%). ^{1}H NMR (250 MHz, Acetone-d_6) δ 7.30 (s, 1H), 7.35 (d, J = 7 Hz, 1H), 7.45 (t, J = 8 Hz, 3H), 7.68 (t, J = 8 Hz, 3H), 7.87 (d, J = 7 Hz, 1H), 8.18 (s, 1H); ^{13}C NMR (75.46 MHz, Acetone-d_6) δ 127.7, 128, 128.9, 129.6, 129.6, 133.5, 134, 140.8, 142.1.

Representative Procedure for the Synthesis of Symmetric Model Compounds. *p-Quinquephenyl* (*PPPPP*; ***I***). A 50 mL two-neck flask equipped with magnetic stir bar, reflux con-

Javelin-, Hockey Stick-, and Boomerang-Shaped Liquid Crystals

J. Phys. Chem. B, Vol. 105, No. 37, 2001 **8859**

denser, and argon inlet was charged (under argon atmosphere) with 1,4-dibromobenzene (**5**) (4.08 g, 5 mmol) and 6 mol % tetrakis(triphenylphosphine)palladium(0) (0.69 g, 0.6 mmol). A volume of 10 mL of dimethoxyethane (DME) was added and this yellow solution was stirred for 10 min at room temperature. 4-Biphenylboronic acid (**2**) (2.97 g, 15 mmol) and 10 mL of 2 M Na_2CO_3 were added and this mixture was refluxed under argon atmosphere for 24 h. After cooling to room temperature the reaction mixture was diluted with 50 mL of water and filtered. The solids were washed with acetone and dichloromethane and vacuum-dried overnight at 60 °C. Pure *p*-quinquephenyl (**I**), 1.49 g (78%), was obtained as colorless platelets after three recrystallizations from hot 1,2,4-trichlorobenzene. IR (KBr) ν_{max}: 1476, 1449, 1399, 1001, 818, 754, 687 cm^{-1}.[36] High-resolution MS: (M+) = 382.1725 (theoretical 382.1722), confirmed elemental composition: $C_{30}H_{22}$. Low-resolution MS: 382 (M+), 344, 302, 192, 191, 44. λ_{max} (nm) (CH$_2$Cl$_2$) = 309.4.

Analytical Data. *2,5-Bisbiphenyl-4-yl-thiophene* (*PPTPP*; **IV**). Bright yellow platelets from 1,2,4-trichlorobenzene, yield = 1.7 g (88%); IR (KBr) ν_{max}: 1481, 1443, 1404, 1132, 937, 835, 795, 758, 714, 685 cm^{-1}. High-resolution MS: (M+) = 388.1286 (theoretical 388.1286), confirmed elemental composition: $C_{28}H_{20}S$. Low-resolution MS: (M+): 388 (M+), 194, 44. λ_{max} (nm) (CH$_2$Cl$_2$) = 356.0.

1,3-Bisbiphenyl-4-yl-benzene (*PPMPP*; **XI**). Colorless platelets from 1,2,4-trichlorobenzene, yield = 0.28 g (73%); IR (KBr) ν_{max}: 1591, 1574, 1472, 1379, 1121, 999, 841, 789, 754, 719, 687, 557, 496 cm^{-1}. High-resolution MS: (M+) = 382.1729 (theoretical 382.1722), confirmed elemental composition: $C_{30}H_{22}$. Low-resolution MS: 382 (M+), 191. λ_{max} (nm) (CH$_2$Cl$_2$) = 285.1.

Representative Procedure for the Synthesis of Asymmetric Model Compounds. *2-Terphenyl-4-yl-5-phenyl thiophene* (*PPPTP*; **III**). A 25 mL two-neck flask equipped with magnetic stir bar, reflux condenser, and argon inlet was charged (under argon atmosphere) with 4-bromo-*p*-terphenyl (**4**) (0.21 g, 0.68 mmol) and 5 mol % tetrakis(triphenylphosphine)palladium(0) (0.04 g, 0.03 mmol). A volume of 5 mL of dimethoxyethane (DME) was added and this yellow solution was stirred for 10 min at room temperature. 2-Phenyl-5-thiopheneboronic acid (**12**) (0.14 g, 0.7 mmol) and 5 mL of 2 M Na_2CO_3 were added and this mixture was refluxed under argon atmosphere for 24 h. After cooling to room temperature the reaction mixture was diluted with 20 mL of water and filtered. The solids were washed with acetone and dichloromethane and vacuum-dried overnight at 60 °C. Pure 2-terphenyl-4-yl-5-phenyl thiophene (**III**), 0.23 g (89%), was obtained as yellow platelets after three recrystallizations from hot 1,2,4-trichlorobenzene. IR (KBr) ν_{max}: 1483, 1449, 1398, 822, 799, 751, 748, 721, 687 cm^{-1}. High-resolution MS: (M+) = 388.1281 (theoretical 388.1286), confirmed elemental composition: $C_{28}H_{20}S$. Low-resolution MS: 388 (M+), 194, 44. λ_{max} (nm) (CH$_2$Cl$_2$) = 348.0.

Analytical Data. *3-Terphenyl-4-yl-5-phenyl thiophene* (*PPPT'P*; **V**). Colorless platelets from 1,2,4-trichlorobenzene, yield = 0.23 g (85%); IR (KBr) ν_{max}: 1478, 1447, 1398, 882, 818, 754, 685, 472 cm^{-1}. High-resolution MS: (M+) = 388.1287 (theoretical 388.1286), confirmed elemental composition: $C_{28}H_{20}S$. Low-resolution MS: 388 (M+), 194. λ_{max} (nm) (CH$_2$Cl$_2$) = 299.0.

2-Terphenyl-4-yl-4-phenyl thiophene (*PPPT''P*; **VI**). Colorless platelets from 1,2,4-trichlorobenzene, yield = 0.18 g (69%); IR (KBr) ν_{max}: 1478, 1447, 1398, 882, 816, 760, 725, 691, 472 cm^{-1}. High-resolution MS: (M+) = 388.1277 (theoretical

388.1286), confirmed elemental composition: $C_{28}H_{20}S$. Low-resolution MS: 388 (M+), 343, 194, 44. λ_{max} (nm) (CH$_2$Cl$_2$) = 326.0.

2-Quaterphenyl-4-yl-thiophene (*PPPPT*; **II**). Slight yellow platelets from 1,2,4-trichlorobenzene, yield = 0.043 g (62%); IR (KBr) ν_{max}: 1479, 1425, 1398, 995, 843, 810, 760, 681 cm^{-1}. High-resolution MS: (M+) = 388.1283 (theoretical 388.1286), confirmed elemental composition: $C_{28}H_{20}S$. Low-resolution MS: 388 (M+), 344, 194, 44. λ_{max} (nm) (CH$_2$Cl$_2$) = 324.0.

2-Terphenyl-4-yl-5-phenyl-1,3,4-oxadiazole (*PPPOP*; **VII**). Colorless platelets from CH$_2$Cl$_2$, yield = 0.54 g (72%); IR (KBr) ν_{max}: 1610, 1578, 1546, 1481, 1448, 1400, 1082, 1069, 1002, 964, 922, 828, 766, 739 cm^{-1}. Low-resolution MS: 374 (M+), 345, 317, 306, 241, 226, 187, 165, 153. TLC (CH$_2$Cl$_2$), one spot (silica gel, t_r = 0.1). λ_{max} (nm) (CH$_2$Cl$_2$) = 311.0.

2-Phenyl-5-terphenyl-4-yl-oxazole (*PPPO'P*; **VIII**). Colorless platelets from CH$_2$Cl$_2$, yield = 0.18 g (75%); IR (KBr) ν_{max}: 1541, 1481, 1449, 1401, 1136, 952, 844, 830, 823, 767, 732, 711, 692 cm^{-1}. Low-resolution MS: 373 (M+), 345, 317, 306, 241, 228, 187, 173, 165. TLC (CH$_2$Cl$_2$), one spot (silica gel, t_r = 0.28). λ_{max} (nm) (CH$_2$Cl$_2$) = 335.1.

2-Terphenyl-4-yl-5-phenyl-oxazole (*PPPO''P*; **IX**). Colorless platelets from CH$_2$Cl$_2$, yield = 0.18 g (72%); IR (KBr) ν_{max}: 1480, 1399, 1260, 1098, 1021, 950, 844, 826, 768, 743, cm^{-1}. Low-resolution MS: 373 (M+), 345, 317, 306, 241, 228, 187, 173, 165. TLC (CH$_2$Cl$_2$), one spot (silica gel, t_r = 0.3). λ_{max} (nm) (CH$_2$Cl$_2$) = 329.0.

1-Terphenyl-4-yl-3-phenyl benzene (*PPPMP*; **X**). Colorless platelets from 1,2,4-trichlorobenzene, yield = 0.13 g (54%); IR (KBr) ν_{max}: 1483, 1470, 1387, 1074, 1001, 824, 795, 752, 692, 610, 486 cm^{-1}. High-resolution MS: (M+) = 382.1719 (theoretical 382.1722), confirmed elemental composition: $C_{30}H_{22}$. Low-resolution MS: 382 (M+), 191. λ_{max} (nm) (CH$_2$Cl$_2$) = 300.0.

References and Notes

(1) (a) Collings, P. J.; Patel, J. S. Introduction to the Science and Technology of Liquid Crystals. In *Handbook of Liquid Crystal Research*; Collings, P. J., Patel, J. S., Eds.; Oxford University Press: New York, 1997; Chapter 1. (b) Collings, P. J.; Hird, M. *Introduction to Liquid Crystals, Chemistry and Physics*; Taylor and Francis: Bristol, 1997; Chapter 3.

(2) Vorländer, D. Z. *Phys. Chem.* **1927**, *449*, 126.

(3) (a) Irvine, P. A.; Wu, D. C.; Flory, P. J. *J. Chem. Soc., Faraday Trans. 1* **1984**, *80*, 1795; (b) Flory, P. J.; Irvine, P. A. *J. Chem. Soc., Faraday Trans. 1* **1984**, *80*, 1807; (c) Irvine, P. A.; Flory, P. J. *J. Chem. Soc., Faraday Trans. 1* **1984**, *80*, 1821.

(4) SPARTAN, version 5.0; Wave function Inc.: Irvine, CA, 1997.

(5) Joule, J. A.; Mills, K.; Smith, G. F. *Heterocyclic Chemistry*; Chapman and Hall: New York, 1995; Chapter 5.

(6) Gronowitz, S.; Hörnfeldt, A.-B. Physical Properties of Thiophene Derivatives. In *The Chemistry of Heterocyclic Compounds*; Taylor, E. C., Ed.; Wiley: New York, 1991; Vol. 44, Part 4, Chapter 1, p 13.

(7) Hedrick, J. L. *Polym. Bull.* **1991**, *25*, 543.

(8) Lakhan, R.; Ternai, B. Advances in Oxazole Chemistry. In *Advances in Heterocyclic Chemistry*; Katritzky, A. R., Boulton, A. J., Eds., Academic Press: New York, 1974; Vol. 17.

(9) Clapp, L. B. 1,2,4-Oxadiazoles. In *Advances in Heterocyclic Chemistry*; Katritzky, A. R., Boulton, A. J., Eds.; Academic Press: New York, 1974; Vol. 20.

(10) Gilchrist, T. L. *Heterocyclic Chemistry*; John Wiley & Sons: New York, 1985; Chapter 7.

(11) Hill, J. 1,3,4-Oxadiazoles. In *Comprehensive Heterocyclic Chemistry*; Potts, K. T., Ed.; Pergamon Press: New York, 1984; Vol. 6, Part 4B, Chapter 4.23, p 428.

(12) Silverman, L.; Trego, K.; Houk, W.; Shideler, M. E. *J. Appl. Chem.* **1958**, *8*, 616.

(13) Ibuki, E.; Ozasa, S.; Murai, K. *Bull. Chem. Soc. Jpn.* **1975**, *48*, 1868.

(14) Ozasa, S.; Hatada, N.; Fujioka, Y.; Ibuki, E. *Bull. Chem. Soc. Jpn.* **1980**, *53*, 2610.

(15) Hird, M.; Gray, G. W.; Toyne, K. J. *Mol. Cryst. Liq. Cryst.* **1991**, *206*, 187.

(16) Gjøs, N.; Gronowitz, S. *Acta Chem. Scand.* **1972**, *26*, 1851.

(17) Gjøs, N.; Gronowitz, S.; Kellogg, R. M.; Wynberg, H. *J. Org. Chem.* **1967**, *32*, 463.

(18) Wang, R. H. S.; Irick, G. U.S. Patent 4,043,973, 1977.

(19) Hayes, F. N.; Rogers, B. S.; Ott, D. G. *J. Am. Chem. Soc.* **1955**, *77*, 1850.

(20) Lewis, I. C.; Kovac, C. A. *Mol. Cryst. Liq. Cryst.* **1979**, *51*, 173.

(21) Schubert, H.; Sagitdinov, I.; Svetkin, *Z. Chem.* **1975**, *15*, 222.

(22) (a) Baker, K. N.; Fratini, A. V.; Resch, T.; Knachel, H. C.; Adams, W. W.; Socci, E. P.; Farmer, B. L. *Polymer* **1993**, *34*, 1571; (b) Baker, K. N.; Fratini, A. V.; Adams, W. W. *Polymer* **1990**, *31*, 1623.

(23) Niori, T.; Sekine, T.; Watanabe, J.; Furukawa, T.; Takezoe, H. *J. Mater. Chem.* **1996**, *6*, 1231.

(24) (a) Link, D. R.; et al. *Science* **1997,** *278*, 1924; (b) Thisayukta, J.; et al. *J. Am. Chem. Soc.* **2000**, *122*, 7441.

(25) Cai, R.; Samulski, E. T. *Liq. Cryst.* **1991**, *9*, 617.

(26) (a) Semmler, K.; Dingemans, T. J.; Samulski, E. T. *Liq. Cryst.* **1998**, *24*, 799; (b) Dingemans, T. J.; Samulski, E. T. *Liq. Cryst.* **2000**, *27*, 131.

(27) (a) Wen, X.; Meyer, R. B. *Phys. Rev. Lett.* **1987**, *59*, 1325; (b) Kimura, K.; Tsuchiya, M. *J. Phys. Soc. Jpn.* **1990**, *59*, 3563.

(28) Samulski, E. T. *Isr. J. Chem.* **1983**, *23*, 329.

(29) Wheland, G. W. *Resonance in Organic Chemistry*; Wiley: New York 1955; see also March, J. *Advanced Organic Chemistry*, 4th ed.; Wiley: New York, 1992; pp 40−45.

(30) Dingemans, T. J.; Bacher, A.; Thelakkat, M.; Pedersen, L. G.; Samulski, E. T.; Schmidt, H.-W. *Synth. Met.* **1999**, *105*, 171.

(31) Maier, W.; Saupe, A. *Z. Naturforsch., Teil A* **1958**, *13*, 564; Maier, W.; Saupe, A. *Z. Naturforsch., Teil A* **1959**, *14*, 882; Maier, W.; Saupe, A. *Z. Naturforsch., Teil A* **1960**, *15*, 287.

(32) Vanakaras, A. G.; Photinos, D. J.; Samulski, E. T. *Phys. Rev.* **1999**, *57*, 4875.

(33) Schlosser, M. *Organometallics in Synthesis*; Willey: New York, 1994; p 448.

(34) Gabe, E. J.; Le Page, Y.; Charland, J.-P.; Lee, F. L.; White, P. S. *J. Appl. Crystallogr.* **1989**, *22*, 384.

(35) Wilson, N. K.; Zehr, R. D. *J. Org. Chem.* **1982**, *47*, 1184.

(36) Doss, R. C.; Solomon, P. W. *J. Org. Chem.* **1964**, *29*, 1567.